
BLoB: Bayesian Low-Rank Adaptation by Backpropagation for Large Language Models

Yibin Wang^{*1} Haizhou Shi^{*2} Ligong Han² Dimitris Metaxas² Hao Wang^{†2}

Abstract

Large Language Models (LLMs) often suffer from overconfidence during inference, particularly when adapted to downstream domain-specific tasks with limited data. Previous work addresses this issue by employing approximate Bayesian estimation *after* the LLMs are trained, enabling them to quantify uncertainty. However, such post-training approaches' performance is severely limited by the parameters learned *during* training. In this paper, we go beyond post-training Bayesianization and propose **Bayesian Low-Rank Adaptation by Backpropagation (BLoB)**, an algorithm that continuously and jointly adjusts both the mean and covariance of LLM parameters throughout the whole fine-tuning process. Our empirical results verify the effectiveness of BLoB in terms of generalization and uncertainty estimation, when evaluated on both in-distribution and out-of-distribution data.

1 Introduction

Despite the recent advancements in Large Language Models (LLMs) [9, 99, 98, 65, 15, 4, 88, 89, 76, 12, 1, 70], addressing the challenges of reliability and responsibility remains imperative [42]. LLMs often produce overconfident responses detached from factual grounding, posing potential harm to users [3, 100, 44, 43, 84, 50, 7, 110, 104, 112, 33, 67, 107, 45]. Therefore, accurately estimating response confidence (or uncertainty) is crucial to preemptively intervene before harm occurs. Current research predominantly focuses on eliciting the internal capability of uncertainty estimation of LLMs. For example, studies suggest that verbalized uncertainty yields better-calibrated results compared to conditional probability [84, 45].

While effective, the aforementioned methods do not offer a universal solution for expressing LLM uncertainty across all scenarios, especially when adapted to domain-specific corpora, human preferences, or downstream tasks [44]. Even a well-calibrated LLM may struggle to estimate uncertainty during fine-tuning due to catastrophic forgetting of general knowledge [82]. Moreover, when applied to limited-scale downstream tasks, excessively over-parameterized LLMs can rapidly overfit, leading to overconfidence. Thus, enabling accurate uncertainty estimation of LLMs is vital for their reliable and responsible deployment.

Bayesian methods emerge as a natural solution for learning uncertainty estimation abilities among their counterparts [85, 11, 94, 29, 46, 51, 61, 58, 95, 20, 103]. These methods model predictive uncertainty $P(\mathbf{y}|\mathbf{x}, \mathcal{D})$ by marginalizing the posterior parameter distribution $P(\boldsymbol{\theta}|\mathcal{D})$ after observing the dataset \mathcal{D} :

$$P(\mathbf{y}|\mathbf{x}, \mathcal{D}) = \int P(\mathbf{y}|\mathbf{x}, \boldsymbol{\theta})P(\boldsymbol{\theta}|\mathcal{D})d\boldsymbol{\theta}. \quad (1)$$

However, adapting the Bayesian framework to LLMs poses significant challenges. LLM architectures typically incorporate complex components, including non-linear activation functions, rendering exact

^{*}Equal Contribution. ¹Huazhong University of Science and Technology ²Rutgers University.
[†]Correspondence to: Hao Wang <hw488@cs.rutgers.edu>.

Bayesian inference of parameter posteriors intractable, i.e., unable to compute the integral precisely. Consequently, finding an accurate approximation algorithm for the true posterior distribution becomes a primary challenge. Additionally, modeling parameter posterior distributions demands extra memory space, imposing a prohibitive burden on systems due to the massive scale of LLMs.

Contemporary methods leverage Parameter-Efficient Fine-Tuning (PEFT) to reduce the number of tunable parameters, thus alleviating computational and storage resource burdens [23, 41, 26, 113, 56, 53]. Built on this, recent research explores Bayesianizing only the PEFT module during fine-tuning to calibrate LLMs [8, 96, 108, 68], somewhat relieving the burden of introducing more parameters for posterior approximation. However, initial investigations suggest that straightforward combinations of PEFT and basic Bayesian techniques like Monte-Carlo Dropout (MCD, [29]) or Deep Ensemble (ENS, [51, 8, 96]) yield only marginal improvements in generalization and uncertainty estimation. The most promising results to date involve Kronecker factorized Laplace approximation, applied after maximum a posteriori (MAP) estimation provided by any optimization algorithm [108]. Nevertheless, we argue that such post-training procedures bifurcate posterior approximation into two stages, inevitably leading to suboptimal estimation.

To address this challenge, we propose **Bayesian Low-Rank Adaptation by Backpropagation (BLoB)**, a Bayesian Deep Learning framework for fine-tuning LLMs with LoRA. BLoB jointly estimates the low-rank variational distributions’ mean and covariance throughout the entire fine-tuning stage via backpropagation. Unlike methods relying on post-training approximation, BLoB enables simultaneous estimation of both the parameter mode (i.e., the mean if one assumes Gaussian distributions) and the parameter variance. Random sampling of model parameters based on variance estimation can enhance mode estimation. It thereby improves model performance in terms of accuracy and uncertainty estimation on both in-distribution and out-of-distribution datasets, as verified by our extensive experiments across multiple datasets. In summary, our contributions are:

- We propose a principled Bayesianization framework for Low-Rank Adaptation (LoRA) in Large Language Models (LLMs) by assuming that full weights’ approximate posterior distribution has a low-rank structure containing a linear combination of independent Gaussian distributions.
- We show that, under mild conditions, optimization of the full-weight variational distribution can be done efficiently in the low-rank space of the weight update matrices.
- We introduce BLoB, a variational Bayesian low-rank adaptation framework for LLMs that jointly learns the mean and covariance of the variational distribution during fine-tuning.
- Extensive evaluations demonstrate the superiority of BLoB in terms of generalization and uncertainty estimation across different scenarios.

2 Preliminaries

In this section, we describe the notation as well as some preliminaries.

Notation. In this paper, scalars are denoted by lowercase letters, vectors by lowercase boldface letters, and matrices by uppercase boldface letters. Probability, expectation, and the dataset are denoted by P , \mathbb{E} , and \mathcal{D} , respectively. We use $[m] = \{1, 2, \dots, m\}$ to denote the set of consecutive integer numbers starting from 1 and ending at m . For a matrix $\mathbf{X} = [\mathbf{x}_1, \dots, \mathbf{x}_n] \in \mathbb{R}^{m \times n}$, we use $\text{vec}(\mathbf{X}) = [\mathbf{x}_1^\top, \mathbf{x}_2^\top, \dots, \mathbf{x}_n^\top]^\top \in \mathbb{R}^{(mn) \times 1}$ to denote the vectorization operation; we use $\|\mathbf{X}\|_p = \left[\sum_{ij} |X_{ij}|^p \right]^{1/p}$ to define the p -norm of a matrix. We use \otimes and \circ to denote the Kronecker product and the element-wise product, respectively.

2.1 Low-Rank Adaptation (LoRA)

Inspired by the pioneering work on identifying and leveraging the low intrinsic rank of over-parameterized models during fine-tuning [55, 2], Low-Rank Adaptation (LoRA) assumes a low rank for the network’s weight updates [41]. Typically in a single linear layer, LoRA decomposes each update matrix $\Delta \mathbf{W} = \mathbf{B}\mathbf{A}$ into the product of two low-rank matrices, where $\mathbf{B} \in \mathbb{R}^{m \times r}$ and $\mathbf{A} \in \mathbb{R}^{r \times n}$. Here, m , n , and r denote the number of input neurons, output neurons, and the rank of the decomposition, respectively [41]. The forward pass of the linear layer with LoRA is formulated

as:

$$\mathbf{z} = \mathbf{W}_0\mathbf{h} + \Delta\mathbf{W}\mathbf{h} = \mathbf{W}_0\mathbf{h} + \mathbf{B}\mathbf{A}\mathbf{h}, \quad (2)$$

where \mathbf{h} and \mathbf{z} denote the input and output of the layer. Since the rank $r \ll \min\{m, n\}$ is significantly smaller than the numbers of input and output neurons (e.g., $r = 8 \ll m = n = 4096$ in the attention layer [41]), LoRA can drastically reduce the number of trainable parameters by approximately three orders of magnitude compared to full-parameter fine-tuning, while achieving comparable performance to the full-rank fine-tuning. This also leads to a similar reduction in memory consumption for storing optimizer states, thereby reducing the hardware requirements for fine-tuning LLMs to a great extent.

2.2 Variational Bayesian Networks (VBNs)

Bayesian Neural Networks (BNNs) estimate the posterior distributions of network parameters rather than relying on single-point estimates [10, 95]. Due to the intractability of exact inference of the true posterior, Variational Bayesian Networks (VBNs) approximate the true posterior using a variational distribution; this is done by minimizing its KL divergence from the true posterior distribution [39, 30, 11]. Specifically, if the weights \mathbf{W} 's variational distribution $q(\mathbf{W}|\boldsymbol{\theta})$ is parameterized by $\boldsymbol{\theta}$, minimizing the divergence $\text{KL}[q(\mathbf{W}|\boldsymbol{\theta})\|P(\mathbf{W}|\mathcal{D})]$ is equivalent to minimizing the following variational free energy with respect to $\boldsymbol{\theta}$ [66, 109, 28]:

$$\min_{\boldsymbol{\theta}} \mathcal{F}(\mathcal{D}, \boldsymbol{\theta}) \triangleq -\mathbb{E}_{q(\mathbf{W}|\boldsymbol{\theta})}[\log P(\mathcal{D}|\mathbf{W})] + \text{KL}[q(\mathbf{W}|\boldsymbol{\theta}) \| P(\mathbf{W})]. \quad (3)$$

The final formulation of the objective function in Eqn. 3 offers another interpretation beyond minimizing the KL divergence between the variational and true posterior distributions [11]. Specifically, the first term maximizes the likelihood of the data, while the second term regularizes the variational distribution $q(\mathbf{W}|\boldsymbol{\theta})$. We refer to the first term as the likelihood cost and the second term as the complexity cost. Optimizing these two terms involves balancing the expressiveness of the approximate posterior distribution and its simplicity.

Optimizing the first term of Eqn. 3 requires integrating out the parameterized variational distribution, necessitating Monte Carlo gradient estimation [52, 80]. Using this approach, we can incorporate the re-parameterization trick to enable backpropagation of the gradient to the underlying parameter $\boldsymbol{\theta}$ [71, 47, 77]. In Bayes By Backprop (BBB) [11], the variational distribution is further simplified as a diagonal Gaussian $\mathcal{N}(\boldsymbol{\mu}, \boldsymbol{\sigma}^2)$, where $\boldsymbol{\sigma} = \log(1 + \exp(\boldsymbol{\rho}))$ ensures the standard deviation is positive. Then we have the Monte-Carlo estimation of Eqn. 3 that can pass the gradient to $\boldsymbol{\theta}$:

$$\mathcal{F}(\mathcal{D}, \boldsymbol{\theta}) \approx -\frac{1}{n} \sum_{i=1}^n \log P(\mathcal{D}|\mathbf{W}_i) + \frac{1}{n} \sum_{i=1}^n [\log q(\mathbf{W}_i|\boldsymbol{\theta}) - \log P(\mathbf{W}_i)], \quad (4)$$

where $\mathbf{W}_i = \boldsymbol{\mu} + \log(1 + \exp(\boldsymbol{\rho})) \odot \boldsymbol{\epsilon}_i$ is the i -th sample of the weights yielded by parameterization and $\boldsymbol{\epsilon}_i \sim \mathcal{N}(\mathbf{0}, \mathbf{I})$. In BBB, the authors assume the prior distribution $P(\mathbf{W}) = \pi\mathcal{N}(\mathbf{0}, \boldsymbol{\sigma}_1^2) + (1 - \pi)\mathcal{N}(\mathbf{0}, \boldsymbol{\sigma}_2^2)$ to be a mixture of Gaussians. Consequently, they optimize the second term based on weight sampling. In different scenarios, a simpler form of the prior, which allows for a closed-form solution, can also be considered. Although our proposed method is largely based on the existing framework of BBB, trivially combining BBB with LoRA does not yield satisfactory results. It is important to note that our specific designs are necessary to encourage the fast convergence of the variational distribution, which will be introduced later in Sec. 3.

3 Methodology

In this section, we formally introduce our proposed method, **Bayesian Low-Rank Adaptation by Backpropagation (BLoB)**. We begin by discussing the design choices for Bayesianizing LoRA parameters in Sec. 3.1, highlighting the assumptions BLoB makes about the approximate posterior in the full-weight space. Next, in Sec. 3.2, we explore the low-rank structure of the prior distribution in the full-weight space, which in turn motivates our choice of prior distributions in the low-rank parameter space. In Sec. 3.3, we introduce our parameterization method for the variational distributions. In Sec. 3.4, we integrate Flipout [101] into LoRA for improved sampling efficiency and faster convergence. Finally, we present the complete algorithmic description of BLoB in Sec. 3.5. Proof of the theorems and claims in this section can be found in Appendix A.

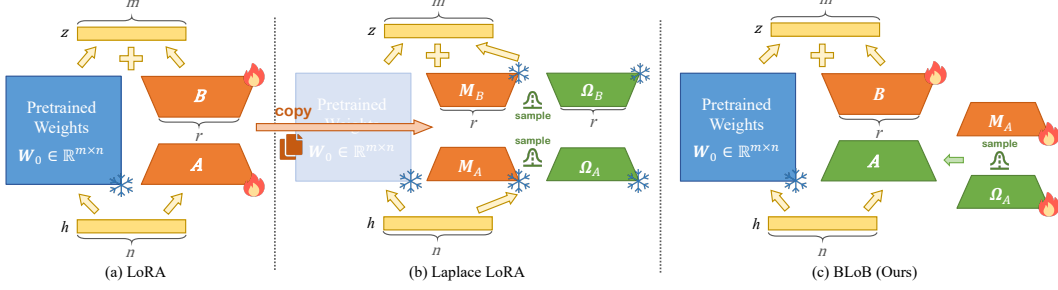


Figure 1: Overview of our Bayesian Low-Rank Adaptation by Backpropagation, i.e., BLoB (right) as well as comparison with existing methods such as LoRA (left) and Laplace LoRA (middle).

3.1 Low-Rank Variational Approximate Posterior Distribution: LoRA Bayesianization

Asymmetric LoRA Bayesianization. In LoRA [41], the weights are treated asymmetrically. A is randomly initialized, usually from the standard normal distribution or using Kaiming initialization, while $B = \mathbf{0}$ is initialized as a zero matrix to ensure that the model fully retains the capabilities of the pre-trained weights at the start of fine-tuning. The trivial solution of estimating the variational approximate posterior for the entire set of LoRA parameters can significantly hinder training convergence. For example, consider the Gaussian posteriors $q(A|\theta) = \mathcal{N}(A|M_A, \Omega_A^2)$ and $q(B|\theta) = \mathcal{N}(B|\mathbf{0}, \Omega_B^2)$, where Ω_A and Ω_B are variance estimates added to A and B , respectively. Although the expectation $\mathbb{E}_{A,B}[(W_0 + BA)x] = W_0x + \mathbb{E}_{A,B}[BAx] = W_0x$ preserves the functionality of the pre-trained model, accurate estimation requires an impractically large number of weight samples. Such variational distributions lead to significant fluctuations during the early stages of fine-tuning, unless the initial variance of B , $\Omega_B \rightarrow \mathbf{0}^+$, is intentionally minimized towards zero. Therefore, we take an *asymmetric* approach to initialize $\Omega_B = \mathbf{0}$ and keep it fixed throughout the fine-tuning process. This, in effect, gives up Bayesian modeling of the B component and focuses only on the posterior of A in LoRA, as shown in Fig. 1.

Additional Advantages. In addition to reducing sampling noise and improving convergence speed, our Bayesianization design has two further advantages. First, compared to modeling the variational distributions of both A and B , our approach significantly reduces additional memory cost by approximately 50% per layer. Second, our design is equivalent to finding a posterior estimate for the full-weight matrix with a low-rank structure. For instance, by assuming a deterministic B and Bayesianizing $P(A|\theta) = \mathcal{N}(A|M, \Omega^2)$, each element of the full weight matrix W_{ij} is calculated as

$$W_{ij} = W_{0,ij} + \sum_{k=1}^r B_{ik}A_{kj}, \quad (5)$$

where $A_{kj} \sim \mathcal{N}(M_{kj}, \Omega_{kj}^2)$ is drawn independently $\forall k \in [r]$. It is noteworthy that due to the low-rank structure defined in Eqn. 5, the full-weight parameters of W are no longer independent from each other. The correlation among them can be reflected by the following theorem:

Theorem 3.1 (Variational Distribution of the Full-Weight Matrix in BLoB). *With the pre-trained weight matrix $W_0 \in \mathbb{R}^{m \times n}$ and the low-rank weight update matrix $B \in \mathbb{R}^{m \times r}$, suppose that the variational distribution of the other low-rank update matrix $A \in \mathbb{R}^{r \times n}$ is Gaussian with $q(A|\theta) = \{M, \Omega\} = \prod_{ij} \mathcal{N}(A_{ij}|M_{ij}, \Omega_{ij}^2)$, where $M = [M_{ij}] \in \mathbb{R}^{r \times n}$ and $\Omega = [\Omega_{ij}] \in \mathbb{R}^{r \times n}$ are its mean and standard deviation, respectively. The equivalent variational distribution defined on the full weight matrix W as in Eqn. 3 is given by*

$$q(\text{vec}(W)|B, \theta) = \mathcal{N}(\text{vec}(W)|\mu_q, \Sigma_q), \quad (6)$$

$$\text{where } \mu_q = \text{vec}(W_0 + BM), \quad (7)$$

$$\Sigma_q = [I_n \otimes B] \cdot [\text{diag}(\text{vec}(\Omega^2))] \cdot [I_n \otimes B^\top]. \quad (8)$$

Theorem 3.1 shows that our asymmetric LoRA Bayesianization is equivalent to using a Gaussian variational distribution for the full weight W (i.e., Eqn. 6), with a flexible covariance matrix (i.e., Eqn. 8), to approximate the posterior distribution of the full weight W .

Remark. *The covariance matrix Σ_q is strictly singular, which consequently inspires us to design a prior $P(W)$ with such low-rank structure in Sec. 3.2. Previous work on low-rank Gaussians typically*

considers covariance with a similar structure $\mathbf{D}^2 + \Sigma_q$, where \mathbf{D} is diagonal [86, 69, 83, 87, 72]. However, sampling from a Gaussian with this structure requires sampling noise of the same shape as the full-weight matrix, which is not parameter-efficient; we therefore do not adopt this in our work.

3.2 Low-Rank Prior Distribution

In Eqn. 3, optimizing the KL divergence between the variational and prior distributions in the space of full weights can be burdensome. Therefore, we assume the prior distribution of the full weights to be a low-rank Gaussian, with its mean centered at the pre-trained weights $\text{vec}(\mathbf{W}_0)$ and its covariance matrix parameterized by a rank- r' matrix $\tilde{\mathbf{R}} \in \mathbb{R}^{(mn) \times r'}$:

$$\begin{aligned} P(\text{vec}(\mathbf{W})) &= \mathcal{N}(\text{vec}(\mathbf{W}) | \boldsymbol{\mu}_p, \boldsymbol{\Sigma}_p), \\ \text{where } \boldsymbol{\mu}_p &= \text{vec}(\mathbf{W}_0), \\ \boldsymbol{\Sigma}_p &= \tilde{\mathbf{R}}\tilde{\mathbf{R}}^\top. \end{aligned} \quad (9)$$

Assuming a low-rank prior distribution and designing an appropriate $\tilde{\mathbf{R}}$ allows us to optimize the KL divergence in the decomposed low-rank weight space, as suggested by the following theorem.

Theorem 3.2 (Efficient Computation of Full-Weight KL Divergence). *Suppose the pre-trained weights \mathbf{W}_0 , update matrix \mathbf{B} , and the variational distribution $q(\mathbf{A}|\boldsymbol{\theta})$ are defined as in Theorem 3.1, and the prior distribution of the full-weight matrix $P(\text{vec}(\mathbf{W}))$ is defined as Eqn. 9. Consider the Gaussian prior distribution $P(\mathbf{A}) = \prod_{ij} \mathcal{N}(A_{ij} | 0, \sigma_p^2)$; we then have:*

$$\text{KL}[q(\text{vec}(\mathbf{W}) | \mathbf{B}, \boldsymbol{\theta}) \| P(\text{vec}(\mathbf{W}))] = \text{KL}[q(\mathbf{A} | \boldsymbol{\theta}) \| P(\mathbf{A})], \quad (10)$$

if $\tilde{\mathbf{R}} = [\sigma_p \mathbf{I}_n \otimes \mathbf{R}]$, where \mathbf{R} satisfies $\mathbf{R}\mathbf{R}^\top = \mathbf{B}\mathbf{B}^\top$.

Theorem 3.2 shows that with a proper $\tilde{\mathbf{R}}$, one can compute the KL divergence for the high-dimensional full weight $\text{vec}(\mathbf{W})$ simply by computing the KL divergence for \mathbf{A} , which is much lower-dimension, more parameter-efficient, more memory-efficient, and faster.

Concretely, we assume that the prior distribution in BLoB follows the low-rank structure described in Theorem 3.2 and minimize the KL divergence term for the low-rank component \mathbf{A} using its analytical solution in Eqn. 3:

$$\min \text{KL}[q(\mathbf{A} | \boldsymbol{\theta} = \{M, \Omega\}) \| P(\mathbf{A})] = \frac{1}{2\sigma_p^2} (\|M\|_2^2 + \|\Omega\|_2^2) - \sum_{ij} \log \Omega_{ij}. \quad (11)$$

3.3 Parameterization of the Low-Rank Variational Distribution

The parameterization of the Gaussian variational distribution $q(\mathbf{A}|\boldsymbol{\theta})$ significantly affects the convergence speed of the KL term in Eqn. 11. The mean matrix M of $q(\mathbf{A}|\boldsymbol{\theta})$ has no additional constraints, we therefore parameterize it directly as the output of a neural network. Each entry of $q(\mathbf{A}|\boldsymbol{\theta})$'s diagonal covariance matrix Ω (i.e., standard deviation) is non-negative; we therefore use element-wise parameterization $\Omega_{ij} = G_{ij}^2$, where $\mathbf{G} = [G_{ij}] \in \mathbb{R}^{r \times n}$ is the real parameter matrix that determines the standard deviation Ω . Since Ω is usually initialized with small positive values close to zero, our parameterization method provides large gradients initially, contributing to the rapid decrease of the KL term. We further show, both theoretically and empirically, that our parameterization method, unlike BBB's softplus function $\log(1 + \exp(\cdot))$, is crucial for the fast convergence of Ω when $q(\mathbf{A}|\boldsymbol{\theta})$ is close to the prior distribution $P(\mathbf{A})$ (see more analysis in Appendix A.2).

3.4 On Improving the Sample Efficiency of BLoB

Improving Sample Efficiency with Flipout. One main challenge in estimating the variational distribution (i.e., the approximate posterior) during fine-tuning lies in the sample efficiency of the weights [102, 25, 58]. During mini-batch stochastic gradient descent, a batch of examples typically share the same weights drawn from the variational distribution. This can lead to slow convergence of the likelihood cost in Eqn. 3. Drawing inspiration from [101], we introduce the technique of flipout to speed up the sampling procedure of our low-rank variational distributions $q(\mathbf{A}|\boldsymbol{\theta})$.

LoRA Flipout. Unlike the original approach, which applies rank-1 random flipping to the full weights, we apply flipout exclusively to the low-rank component \mathbf{A} . Specifically, suppose we have a

Algorithm 1 Bayesian Low-Rank Adaptation by Backpropagation (BLoB)

Require: dataset \mathcal{D} , pre-trained weight \mathbf{W}_0 , low-rank component \mathbf{B} , $\boldsymbol{\theta} = \{\mathbf{M}, \mathbf{G}\}$ for parameterizing the mean and variance of \mathbf{A} ;

Require: prior standard deviation σ_p , initialization hyperparameter ϵ , number of input features n ;

Require: number of samples during training K , number of iterations T , learning rate η ;

- 1: $\mathbf{G} \sim \mathcal{U}(\frac{\epsilon}{\sqrt{2}}, \epsilon)$, $\mathbf{M} \sim \mathcal{U}(-\sqrt{\frac{6}{n}}, \sqrt{\frac{6}{n}})$ ▷ Initialization of \mathbf{A} 's parameters.
 - 2: $\mathbf{B} \leftarrow \mathbf{0}$ ▷ Initialization of \mathbf{B} .
 - 3: **for** $t = 1, \dots, T$ **do**
 - 4: Sample a mini-batch of data $\mathcal{D}_t \sim \mathcal{D}$.
 - 5: **for** $k = 1, \dots, K$ **do**
 - 6: Sample batched noise $\mathbf{E}_k \sim \mathcal{N}(\mathbf{0}, \mathbf{I})$. ▷ Sample the noise.
 - 7: Let $\tilde{\mathbf{E}}_k \leftarrow \text{BLoBFlipout}(\mathbf{E}_k)$. ▷ Eqn. 12
 - 8: Let $\mathbf{A}_k = \mathbf{M} + \mathbf{G}^2 \circ \tilde{\mathbf{E}}_k$.
 - 9: **end for**
 - 10: Let $\hat{\mathcal{F}}_t = -\frac{1}{K} \sum_{k=1}^K \log P(\mathcal{D}_t | \mathbf{A}_k, \mathbf{B}) + \frac{1}{2\sigma_p^2} (\|\mathbf{M}\|_2^2 + \|\mathbf{G}\|_2^4) - 2 \sum_{ij} \log G_{ij}$. ▷ Eqn. 13 and 11.
 - 11: Calculate the gradient w.r.t. the parameters:
 $\Delta_{\mathbf{M}} = \partial \hat{\mathcal{F}}_t / \partial \mathbf{M}$, $\Delta_{\mathbf{G}} = \partial \hat{\mathcal{F}}_t / \partial \mathbf{G}$, $\Delta_{\mathbf{B}} = \partial \hat{\mathcal{F}}_t / \partial \mathbf{B}$.
 - 12: Updater the parameters:
 $\mathbf{M} \leftarrow \mathbf{M} - \eta \Delta_{\mathbf{M}}$;
 $\mathbf{G} \leftarrow \mathbf{G} - \eta \Delta_{\mathbf{G}}$;
 $\mathbf{B} \leftarrow \mathbf{B} - \eta \Delta_{\mathbf{B}}$.
 - 13: **end for**
-

mini-batch of input vectors $\mathbf{H} \in \mathbb{R}^{n \times b}$, where b represents the batch size. We randomly sample two low-rank flipping matrices $\mathbf{S} \in \{-1, +1\}^{n \times b}$ and $\mathbf{T} \in \{-1, +1\}^{b \times r}$. Denoting as \mathbf{E} the weight noise sampled for this mini-batch, the batched output \mathbf{Z} after applying flipout is then

$$\mathbf{Z} = \mathbf{W}_0 \mathbf{H} + \mathbf{B}(\mathbf{M} \mathbf{H} + [(\mathbf{E} \circ \boldsymbol{\Omega})(\mathbf{H} \circ \mathbf{S})] \circ \mathbf{T}), \quad (12)$$

where \circ denotes the element-wise product (see Appendix A.3 for derivation). It is crucial that the independent noises added to the low-rank weight noise $\Delta \mathbf{A} \triangleq \mathbf{E} \circ \boldsymbol{\Omega}$ ensure *sampling independence across examples* within a mini-batch, thereby enhancing the sampling efficiency of the algorithm. This is done without violating the assumptions outlined in Theorem 3.1 and 3.2. Besides, due to the low-rank structure of our Bayesianization method, the computational overhead of employing flipout in BLoB is also minimal.

3.5 BLoB: Final Algorithm

We are now ready to present our full BLoB algorithm. Under the assumptions outlined in Theorem 3.1 and 3.2, optimizing the evidence lower bound on the full weight \mathbf{W} can be efficiently done in the low-rank space, using the following final objective function:

$$\begin{aligned} \mathcal{F}(\mathcal{D}, \mathbf{B}, \boldsymbol{\theta}) &= -\mathbb{E}_{q(\mathbf{W}|\mathbf{B}, \boldsymbol{\theta})}[\log P(\mathcal{D}|\mathbf{W})] + \text{KL}[q(\mathbf{W}|\mathbf{B}, \boldsymbol{\theta}) \parallel P(\mathbf{W})] \\ &= -\mathbb{E}_{q(\mathbf{A}|\boldsymbol{\theta})}[\log P(\mathcal{D}|\mathbf{A}, \mathbf{B})] + \text{KL}[q(\mathbf{A}|\boldsymbol{\theta}) \parallel P(\mathbf{A})], \end{aligned} \quad (13)$$

where $\boldsymbol{\theta} = \{\mathbf{M}, \boldsymbol{\Omega}\}$ denotes the set of the parameters underlying the variational distribution of the low-rank matrix \mathbf{A} . The full algorithmic description of BLoB is shown in Algorithm 1.

4 Experiments

In this section, we compare our BLoB with existing methods on real-world datasets. Sec. 4.1 introduces the experimental settings, including baselines, fine-tuning, and evaluation protocols. We then evaluate BLoB's generalization and uncertainty estimation abilities in both in-distribution (Sec. 4.2) and out-of-distribution scenarios (Sec. 4.3).

Table 1: **Performance of different methods applied to LoRA on Llama2-7B pre-trained weights.** The evaluation is done across six common-sense reasoning tasks with a shared hyper-parameter setting after 5,000 training steps. We use N to represent the number of samples during inference in BLoB. “ \uparrow ” and “ \downarrow ” indicate that higher and lower values are preferred, respectively. **Boldface** and underlining denote the best and the second-best performance, respectively.

Metric	Method	Datasets					
		WG-S [81]	ARC-C [18]	ARC-E [18]	WG-M [81]	OBQA [64]	BoolQ [17]
ACC (\uparrow)	MLE	68.99 \pm 0.58	<u>69.10\pm2.84</u>	85.65 \pm 0.92	74.53 \pm 0.66	81.52 \pm 0.25	86.53 \pm 0.28
	MAP	68.62 \pm 0.71	<u>67.59\pm0.40</u>	<u>86.55\pm0.55</u>	75.61\pm0.71	81.38 \pm 0.65	86.50 \pm 0.41
	MCD [29]	68.12 \pm 1.18	66.44 \pm 4.74	85.65 \pm 1.09	73.73 \pm 1.06	83.00\pm0.99	86.67 \pm 0.23
	ENS [51, 8, 96]	<u>69.57\pm0.66</u>	66.20 \pm 2.01	84.40 \pm 0.81	75.32 \pm 0.21	81.38 \pm 0.91	87.09 \pm 0.11
	BBB [11]	56.54 \pm 7.87	68.13 \pm 1.27	85.86 \pm 0.74	73.63 \pm 2.44	82.06 \pm 0.59	87.21\pm0.22
	LAP [108]	69.20 \pm 1.50	29.73 \pm 12.02	80.05 \pm 0.22	<u>75.55\pm0.36</u>	82.12 \pm 0.67	86.95 \pm 0.09
	BLoB (N=0)	70.89\pm0.82	70.83\pm1.57	86.68\pm0.60	74.55 \pm 1.94	82.73 \pm 0.41	86.80 \pm 0.23
	BLoB (N=5)	66.30 \pm 0.62	67.34 \pm 1.15	84.74 \pm 0.33	72.89 \pm 1.25	81.79 \pm 0.94	86.47 \pm 0.15
	BLoB (N=10)	69.07 \pm 0.34	68.81 \pm 1.09	85.56 \pm 0.35	73.69 \pm 0.17	81.52 \pm 0.74	<u>86.99\pm0.24</u>
	ECE (\downarrow)	MLE	29.83 \pm 0.58	29.00 \pm 1.97	13.12 \pm 1.39	20.62 \pm 0.74	12.55 \pm 0.46
MAP		29.76 \pm 0.87	29.42 \pm 0.68	12.07 \pm 0.55	23.07 \pm 0.14	13.26 \pm 0.82	3.16 \pm 0.23
MCD [29]		30.58 \pm 1.08	31.13 \pm 5.50	13.23 \pm 0.85	21.26 \pm 0.78	14.45 \pm 0.84	3.13 \pm 0.09
ENS [51, 8, 96]		28.52 \pm 0.55	29.16 \pm 2.37	12.57 \pm 0.58	20.86 \pm 0.43	15.34 \pm 0.27	9.61 \pm 0.24
BBB [11]		21.81 \pm 12.95	26.23 \pm 1.47	12.28 \pm 0.58	15.76 \pm 4.71	11.38 \pm 1.07	3.74 \pm 0.10
LAP [108]		4.15\pm1.12	14.24 \pm 1.65	33.29 \pm 0.57	7.40 \pm 0.27	8.70 \pm 1.77	1.30\pm0.33
BLoB (N=0)		20.62 \pm 0.83	20.61 \pm 1.16	9.43 \pm 0.38	11.23 \pm 0.69	8.36 \pm 0.38	2.46 \pm 0.07
BLoB (N=5)		10.89 \pm 0.83	<u>11.22\pm0.35</u>	<u>6.16\pm0.23</u>	<u>4.51\pm0.35</u>	3.40\pm0.57	1.63 \pm 0.35
BLoB (N=10)		<u>9.35\pm1.37</u>	9.59\pm1.88	3.64\pm0.53	3.01\pm0.12	<u>3.77\pm1.47</u>	<u>1.41\pm0.19</u>
NLL (\downarrow)		MLE	3.17 \pm 0.37	2.85 \pm 0.27	1.17 \pm 0.13	0.95 \pm 0.07	0.73 \pm 0.03
	MAP	2.46 \pm 0.34	2.66 \pm 0.11	0.90 \pm 0.05	1.62 \pm 0.29	0.75 \pm 0.01	0.33 \pm 0.00
	MCD [29]	2.60 \pm 0.39	3.11 \pm 0.53	1.16 \pm 0.04	0.97 \pm 0.06	1.06 \pm 0.08	0.33 \pm 0.00
	ENS [51, 8, 96]	2.71 \pm 0.08	2.46 \pm 0.22	0.82 \pm 0.03	1.25 \pm 0.03	1.06 \pm 0.04	0.57 \pm 0.02
	BBB [11]	1.40 \pm 0.55	2.23 \pm 0.04	0.91 \pm 0.06	0.84 \pm 0.15	0.66 \pm 0.05	0.31\pm0.00
	LAP [108]	0.63\pm0.00	1.53 \pm 0.01	1.38 \pm 0.01	0.57 \pm 0.01	1.00 \pm 0.00	0.45 \pm 0.00
	BLoB (N=0)	0.91 \pm 0.10	1.19 \pm 0.02	0.56 \pm 0.01	0.60 \pm 0.01	0.56 \pm 0.02	0.32 \pm 0.00
	BLoB (N=5)	<u>0.68\pm0.01</u>	<u>0.90\pm0.01</u>	<u>0.46\pm0.02</u>	<u>0.56\pm0.01</u>	<u>0.53\pm0.01</u>	<u>0.32\pm0.00</u>
	BLoB (N=10)	0.63\pm0.01	0.78\pm0.02	0.40\pm0.01	0.54\pm0.00	0.50\pm0.01	0.31\pm0.00

4.1 Settings

Fine-tuning and Evaluation. We implement BLoB in the PEFT library [63] and fine-tune the LLaMA2-7B [89] model on common-sense reasoning tasks. Following Laplace-LoRA [108], we apply LoRA to the output layer as well as the queries and values of all the attention layers. For hyperparameters, we strictly adhere to the default settings in the PEFT library and the original LoRA paper [63, 41] to ensure maximal reproducibility. This includes the number of training steps, learning rate, and LoRA rank r (see Appendix B.1 for details). For common-sense reasoning tasks, we select the next token logits corresponding to possible answers from each dataset and fine-tune the LLM to maximize the likelihood of the correct token. For evaluation, in addition to Accuracy (ACC), we use Expected Calibration Error (ECE [31]) and Negative Log-Likelihood (NLL) to assess the models’ uncertainty estimation ability (see Appendix B.2 for details).

Baselines and Implementation Details. We compare BLoB with state-of-the-art uncertainty estimation methods applied to the LoRA adapters of LLMs, including Maximum Likelihood Estimation (MLE) [41], Maximize A Posteriori (MAP), Monte-Carlo Dropout (MCD) [29], Bayes By Backprop (BBB) [11], Deep Ensemble (ENS) [51, 8, 96], and the latest Laplace-LoRA (LAP) [108].

For MLE, we use the LoRA implementation. For MAP, we use a weight decay rate of $1e - 5$. For MCD, we use an ensemble of 10 LoRAs with a dropout rate of $p = 0.1$. For ENS, we independently fine-tune 3 LoRAs and average their logits during evaluation. For BBB, we adopt the default settings from the Bayesian-Torch library [48] and only Bayesianize the A matrix, similar to BLoB. We re-implement LAP and apply it to the MAP checkpoints. We keep all BLoB-specific hyperparameters consistent across all datasets. Typically, we set the number of samples $K = 1$ during training for all our BLoB experiments, which highlights BLoB’s sampling efficiency. As shown in Table 1, we also report BLoB’s performance with different numbers of samples during Bayesian inference, where $N = 0$ indicates directly using the mean of the weight distribution for prediction.

Table 2: **Performance on in-distribution and out-of-distribution datasets.** All the uncertainty estimation methods are applied to the LoRA adapter added upon the pre-trained Llama2-7B weights.

Metric	Method	Datasets				
		<i>In-Dist.</i>	<i>Smaller Dist. Shift</i>		<i>Larger Dist. Shift</i>	
		OBQA [64]	ARC-C [18]	ARC-E [18]	Chem [38, 37]	Phy [38, 37]
ACC (\uparrow)	MLE	81.52 \pm 0.25	66.20 \pm 0.87	75.12 \pm 0.85	40.62 \pm 2.25	28.82 \pm 1.30
	MAP	81.38 \pm 0.91	69.59 \pm 0.33	75.47 \pm 0.73	44.79\pm0.00	28.47 \pm 1.20
	MCD [29]	83.00\pm0.99	69.03 \pm 0.70	76.00 \pm 1.58	42.71 \pm 0.01	29.17 \pm 4.54
	ENS [51, 8, 96]	81.38 \pm 0.65	67.34 \pm 0.70	75.18 \pm 2.03	43.75 \pm 1.04	30.56 \pm 2.62
	BBB [11]	82.06 \pm 0.59	67.25 \pm 1.18	75.83 \pm 0.75	42.36 \pm 0.49	30.21 \pm 2.25
	LAP [108]	82.76 \pm 0.71	70.95\pm0.48	74.94 \pm 1.16	42.36 \pm 1.77	31.60 \pm 0.49
	BLoB (N=0)	82.73 \pm 0.41	69.93 \pm 1.20	76.88\pm0.41	41.67 \pm 2.25	31.94 \pm 1.77
	BLoB (N=5)	81.79 \pm 0.94	68.36 \pm 1.39	75.82 \pm 1.15	40.62 \pm 3.07	32.64\pm0.98
	BLoB (N=10)	81.52 \pm 0.74	67.71 \pm 1.13	76.37 \pm 0.80	44.79\pm1.47	31.60 \pm 2.73
	ECE (\downarrow)	MLE	12.55 \pm 0.46	22.20 \pm 0.39	16.47 \pm 0.86	21.72 \pm 0.30
MAP		15.34 \pm 0.27	19.31 \pm 1.46	15.68 \pm 0.51	17.55 \pm 1.95	30.25 \pm 2.18
MCD [29]		14.45 \pm 0.84	19.54 \pm 0.33	15.32 \pm 1.16	17.9 \pm 0.63	29.53 \pm 4.20
ENS [51, 8, 96]		13.26 \pm 0.82	7.59 \pm 1.43	6.44 \pm 0.83	12.04 \pm 4.57	17.52 \pm 1.28
BBB [11]		11.38 \pm 1.07	19.90 \pm 0.66	13.41 \pm 0.85	15.67 \pm 1.23	26.10 \pm 4.76
LAP [108]		8.83 \pm 1.14	5.84\pm0.64	8.51 \pm 1.06	13.30 \pm 2.31	13.91\pm0.90
BLoB (N=0)		8.36 \pm 0.38	14.00 \pm 1.02	10.70 \pm 0.39	15.05 \pm 0.77	22.90 \pm 2.27
BLoB (N=5)		3.40\pm0.57	9.76 \pm 0.71	5.96 \pm 0.93	14.33 \pm 1.55	18.15 \pm 1.96
BLoB (N=10)		3.77 \pm 1.47	9.55 \pm 0.40	5.48\pm1.27	9.77\pm1.35	18.29 \pm 1.35
NLL (\downarrow)		MLE	0.73 \pm 0.03	1.16 \pm 0.00	0.92 \pm 0.03	1.56 \pm 0.06
	MAP	1.06 \pm 0.04	1.10 \pm 0.07	0.93 \pm 0.04	1.55 \pm 0.06	1.65 \pm 0.03
	MCD [29]	1.06 \pm 0.08	1.08 \pm 0.01	0.88 \pm 0.03	1.59 \pm 0.07	1.67 \pm 0.05
	ENS [51, 8, 96]	0.75 \pm 0.01	0.86 \pm 0.01	0.69 \pm 0.03	1.28\pm0.00	1.39 \pm 0.03
	BBB [11]	0.66 \pm 0.05	1.06 \pm 0.01	0.79 \pm 0.02	1.49 \pm 0.05	1.62 \pm 0.06
	LAP [108]	1.00 \pm 0.01	1.29 \pm 0.00	1.23 \pm 0.01	1.32 \pm 0.01	1.36\pm0.01
	BLoB (N=0)	0.56 \pm 0.02	0.89 \pm 0.02	0.67 \pm 0.02	1.44 \pm 0.00	1.53 \pm 0.02
	BLoB (N=5)	0.53 \pm 0.01	0.85 \pm 0.00	0.64 \pm 0.01	1.39 \pm 0.02	1.48 \pm 0.01
	BLoB (N=10)	0.50\pm0.01	0.83\pm0.01	0.60\pm0.01	1.38 \pm 0.01	1.46 \pm 0.02

4.2 Results on In-distribution Datasets

We fine-tune Llama2-7B on six common-sense reasoning tasks: Winogrande-small (WG-S), Winogrande-medium (WG-M) [81], ARC-Challenge (ARC-C) [18], ARC-Easy (ARC-E) [18], OpenBookQA (OBQA) [64], and BoolQ [17]. For all baseline methods, using the same pre-trained LLM backbone, we maintain consistent hyperparameters across all datasets and do not use additional validation sets to achieve higher performance (See Appendix B.3 for detailed settings).

Table 1 shows the performance of BLoB compared to the baselines, including ACC, ECE, and NLL, on the in-distribution test set with the pre-trained Llama2-7B model. The high ECE and NLL for MLE indicate overconfidence in LLMs during conventional fine-tuning, except for BoolQ due to its large dataset size. Simple but popular baselines like MAP, MCD, and ENS show mixed results in terms of NLL and/or ECE, highlighting the challenge of uncertainty estimation during LLM fine-tuning. LAP, the most competitive post-training baseline for uncertainty estimation, significantly reduces NLL and ECE on some datasets but lacks consistent performance, as indicated by its failures on ARC-C and ARC-E. BBB mitigates the overconfidence issue in LLMs across almost all datasets, showcasing the advantage of jointly optimizing the mean and covariance of the variational weight distributions during fine-tuning. However, there remains considerable room for improvement.

BLoB consistently achieves better or comparable performance across all datasets. With the number of samples during inference set to $N = 10$, the same as MCD, BLoB provides the best uncertainty estimation performance, significantly reducing NLL and ECE, and greatly mitigating overconfidence while maintaining comparable or better ACC than MLE. Even with half the number of samples, $N = 5$, BLoB still delivers performance comparable to that of $N = 10$ and outperforms other baselines on most datasets. Surprisingly, using only the mean of the weight distribution, BLoB achieves significantly higher ACC than other baselines on smaller datasets (WG-S, ARC-C, ARC-E) without a substantial loss in uncertainty estimation quality. This observation further confirms that jointly learning the mean and covariance during fine-tuning can mutually improve their quality.

Besides Llama2-7B, we also include additional results for RoBERTa-base [60] on text classification tasks in Appendix C.1. Our method consistently achieved either the best or runner-up performance across nearly all datasets, demonstrating its versatility across different architectures.

4.3 Results on Out-of-Distribution Datasets

We use models fine-tuned on OBQA [64] to evaluate the generalization ability of different methods under distributional shifts. OBQA consists of multiple-choice elementary-level science questions. We categorize the distributional shifts into two types: *smaller* and *larger* shifts. The ARC [18] dataset, which also consists of multiple-choice science questions, represents a smaller distributional shift. The college-level chemistry and physics subsets of MMLU [38] represent larger distributional shifts.

The results in Table 2 highlight BLoB’s superior OOD generalization ability compared to other methods on both smaller and larger distribution shifts. BLoB achieves the highest accuracy when solely utilizing the mean of the weight distribution in smaller distribution shifts. For larger distribution shifts, incorporating uncertainty through sampling improves model accuracy. Regarding uncertainty estimation, BLoB demonstrates the best or second-best performance in smaller distribution shifts. Although there is a slight performance drop with larger distribution shifts, BLoB remains comparable to baselines such as ENS and LAP.

5 Related Work

Parameter-Efficient Fine-Tuning (PEFT) for LLMs. Due to the prohibitively large size of LLMs, parameter-efficient fine-tuning has become a trending topic. Computational paradigms in this area include adapter-based fine-tuning [40, 36, 79, 74, 62], prompt-based fine-tuning [34, 54, 59, 57, 91, 6], and partial fine-tuning [111, 116, 5, 105, 32]. Among these, LoRA [41] has gained significant attention due to its simplicity and effectiveness. Building on LoRA, numerous studies have aimed to further optimize parameter efficiency when fine-tuning large models [26, 35, 22, 21]. For instance, KronA models weight updates as the Kronecker product of two smaller matrices without decreasing the update rank [26], and SVDiff performs Singular Value Decomposition (SVD) on the original weight matrices, fine-tuning only the singular values [35]. However, in this paper, we focus solely on Bayesianizing LoRA due to its widespread application in existing works. We also note that BLoB can be naturally adapted to handle different LoRA variants.

Uncertainty Estimation in Large Language Models. Large-scale pre-trained models are well-calibrated during pre-training [44], but fail to accurately express predictive uncertainty during inference [3, 100, 44, 43, 84], especially after fine-tuning [8, 96, 108, 68]. This indicates that measures effective during pre-training [90, 106, 16, 114, 14] may lose their power of uncertainty estimation after fine-tuning for domain-specific knowledge. To address this issue, [27, 115] define priors and approximate posteriors on the full attention weights during fine-tuning, achieving better uncertainty estimation but at a significant cost in time and space. Consequently, recent work integrates Bayesian methods and PEFT for efficient uncertainty estimation. For instance, [8, 96] train and store multiple copies of different LoRAs, ensembling their outputs during inference to achieve somewhat better results. [108] applies Kronecker factorized Laplace approximation on fine-tuned LoRA. However, such post-training procedures bifurcate posterior approximation into two stages, leading to suboptimal estimation. In contrast, our BLoB enables simultaneous estimation of both the mean and covariance of LLM parameters in a single fine-tuning stage, substantially improving performance.

6 Conclusion

In this work, we propose a principled Bayesianization framework for parameter-efficiently fine-tuning LLMs. Our theoretical analysis shows that a full-weight variational distribution can be efficiently optimized by approximately using a low-rank space of the weight update matrices. Our empirical evaluations corroborate this theoretical insight, demonstrating superior generalization and uncertainty estimation capabilities across diverse scenarios compared to various baseline methods. Building on LoRA, our approach seamlessly integrates with existing LLM architectures while imposing minimal additional memory overhead and training time. Our method highlights that jointly learning the mean and covariance of the variational distribution during fine-tuning can mutually improve both, underscoring the powerful potential of Bayesian methods in enhancing the reliability and generalization of LLMs.

References

- [1] J. Achiam, S. Adler, S. Agarwal, L. Ahmad, I. Akkaya, F. L. Aleman, D. Almeida, J. Altenschmidt, S. Altman, S. Anadkat, et al. Gpt-4 technical report. *arXiv preprint arXiv:2303.08774*, 2023.
- [2] A. Aghajanyan, S. Gupta, and L. Zettlemoyer. Intrinsic dimensionality explains the effectiveness of language model fine-tuning. In *Proceedings of the 59th Annual Meeting of the Association for Computational Linguistics and the 11th International Joint Conference on Natural Language Processing (Volume 1: Long Papers)*, pages 7319–7328, 2021.
- [3] D. Amodei, C. Olah, J. Steinhardt, P. Christiano, J. Schulman, and D. Mané. Concrete problems in ai safety, 2016.
- [4] R. Anil, A. M. Dai, O. Firat, M. Johnson, D. Lepikhin, A. Passos, S. Shakeri, E. Taropa, P. Bailey, Z. Chen, et al. Palm 2 technical report. *arXiv preprint arXiv:2305.10403*, 2023.
- [5] A. Ansell, E. M. Ponti, A. Korhonen, and I. Vulić. Composable sparse fine-tuning for cross-lingual transfer. *arXiv preprint arXiv:2110.07560*, 2021.
- [6] A. Asai, M. Salehi, M. E. Peters, and H. Hajishirzi. Attempt: Parameter-efficient multi-task tuning via attentional mixtures of soft prompts. In *Proceedings of the 2022 Conference on Empirical Methods in Natural Language Processing*, pages 6655–6672, 2022.
- [7] A. Azaria and T. Mitchell. The internal state of an llm knows when its lying. *arXiv preprint arXiv:2304.13734*, 2023.
- [8] O. Balabanov and H. Linander. Uncertainty quantification in fine-tuned llms using lora ensembles. *arXiv preprint arXiv:2402.12264*, 2024.
- [9] S. Biderman, H. Schoelkopf, Q. G. Anthony, H. Bradley, K. O’Brien, E. Hallahan, M. A. Khan, S. Purohit, U. S. Prashanth, E. Raff, et al. Pythia: A suite for analyzing large language models across training and scaling. In *International Conference on Machine Learning*, pages 2397–2430. PMLR, 2023.
- [10] C. M. Bishop. Pattern recognition and machine learning. *Springer google schola*, 2:1122–1128, 2006.
- [11] C. Blundell, J. Cornebise, K. Kavukcuoglu, and D. Wierstra. Weight uncertainty in neural network. In *International conference on machine learning*, pages 1613–1622. PMLR, 2015.
- [12] T. Brown, B. Mann, N. Ryder, M. Subbiah, J. D. Kaplan, P. Dhariwal, A. Neelakantan, P. Shyam, G. Sastry, A. Askell, et al. Language models are few-shot learners. *Advances in neural information processing systems*, 33:1877–1901, 2020.
- [13] T. H. Chan, K. W. Lau, J. Shen, G. Yin, and L. Yu. Adaptive uncertainty estimation via high-dimensional testing on latent representations. In A. Oh, T. Naumann, A. Globerson, K. Saenko, M. Hardt, and S. Levine, editors, *Advances in Neural Information Processing Systems*, volume 36, pages 39975–39993. Curran Associates, Inc., 2023.
- [14] W. Chen and Y. Li. Calibrating transformers via sparse gaussian processes. *arXiv preprint arXiv:2303.02444*, 2023.
- [15] A. Chowdhery, S. Narang, J. Devlin, M. Bosma, G. Mishra, A. Roberts, P. Barham, H. W. Chung, C. Sutton, S. Gehrmann, et al. Palm: Scaling language modeling with pathways. *Journal of Machine Learning Research*, 24(240):1–113, 2023.
- [16] T. Cinquin, A. Immer, M. Horn, and V. Fortuin. Pathologies in priors and inference for bayesian transformers. *arXiv preprint arXiv:2110.04020*, 2021.
- [17] C. Clark, K. Lee, M.-W. Chang, T. Kwiatkowski, M. Collins, and K. Toutanova. BoolQ: Exploring the surprising difficulty of natural yes/no questions. In J. Burstein, C. Doran, and T. Solorio, editors, *Proceedings of the 2019 Conference of the North American Chapter of the Association for Computational Linguistics: Human Language Technologies, Volume 1 (Long and Short Papers)*, pages 2924–2936, Minneapolis, Minnesota, June 2019. Association for Computational Linguistics.

- [18] P. Clark, I. Cowhey, O. Etzioni, T. Khot, A. Sabharwal, C. Schoenick, and O. Tafjord. Think you have solved question answering? try arc, the ai2 reasoning challenge, 2018.
- [19] I. Dagan, O. Glickman, and B. Magnini. The pascal recognising textual entailment challenge. In J. Quiñero-Candela, I. Dagan, B. Magnini, and F. d’Alché Buc, editors, *Machine Learning Challenges. Evaluating Predictive Uncertainty, Visual Object Classification, and Recognising Tectual Entailment*, pages 177–190, Berlin, Heidelberg, 2006. Springer Berlin Heidelberg.
- [20] E. Daxberger, A. Kristiadi, A. Immer, R. Eschenhagen, M. Bauer, and P. Hennig. Laplace redux - effortless bayesian deep learning. In M. Ranzato, A. Beygelzimer, Y. Dauphin, P. Liang, and J. W. Vaughan, editors, *Advances in Neural Information Processing Systems*, volume 34, pages 20089–20103. Curran Associates, Inc., 2021.
- [21] T. Dettmers, A. Pagnoni, A. Holtzman, and L. Zettlemoyer. Qlora: Efficient finetuning of quantized llms. *Advances in Neural Information Processing Systems*, 36, 2024.
- [22] N. Ding, X. Lv, Q. Wang, Y. Chen, B. Zhou, Z. Liu, and M. Sun. Sparse low-rank adaptation of pre-trained language models. *arXiv preprint arXiv:2311.11696*, 2023.
- [23] N. Ding, Y. Qin, G. Yang, F. Wei, Z. Yang, Y. Su, S. Hu, Y. Chen, C.-M. Chan, W. Chen, et al. Parameter-efficient fine-tuning of large-scale pre-trained language models. *Nature Machine Intelligence*, 5(3):220–235, 2023.
- [24] W. B. Dolan and C. Brockett. Automatically constructing a corpus of sentential paraphrases. In *Proceedings of the Third International Workshop on Paraphrasing (IWP2005)*, 2005.
- [25] M. Dusenberry, G. Jerfel, Y. Wen, Y. Ma, J. Snoek, K. Heller, B. Lakshminarayanan, and D. Tran. Efficient and scalable Bayesian neural nets with rank-1 factors. In H. D. III and A. Singh, editors, *Proceedings of the 37th International Conference on Machine Learning*, volume 119 of *Proceedings of Machine Learning Research*, pages 2782–2792. PMLR, 13–18 Jul 2020.
- [26] A. Edalati, M. Tahaei, I. Kobyzev, V. P. Nia, J. J. Clark, and M. Rezagholizadeh. Krona: Parameter efficient tuning with kronecker adapter. *arXiv preprint arXiv:2212.10650*, 2022.
- [27] X. Fan, S. Zhang, B. Chen, and M. Zhou. Bayesian attention modules. *Advances in Neural Information Processing Systems*, 33:16362–16376, 2020.
- [28] K. Friston, J. Mattout, N. Trujillo-Barreto, J. Ashburner, and W. Penny. Variational free energy and the laplace approximation. *Neuroimage*, 34(1):220–234, 2007.
- [29] Y. Gal and Z. Ghahramani. Dropout as a bayesian approximation: Representing model uncertainty in deep learning. In *international conference on machine learning*, pages 1050–1059. PMLR, 2016.
- [30] A. Graves. Practical variational inference for neural networks. *Advances in neural information processing systems*, 24, 2011.
- [31] C. Guo, G. Pleiss, Y. Sun, and K. Q. Weinberger. On calibration of modern neural networks. In *International conference on machine learning*, pages 1321–1330. PMLR, 2017.
- [32] D. Guo, A. M. Rush, and Y. Kim. Parameter-efficient transfer learning with diff pruning. In *Proceedings of the 59th Annual Meeting of the Association for Computational Linguistics and the 11th International Joint Conference on Natural Language Processing (Volume 1: Long Papers)*, pages 4884–4896, 2021.
- [33] N. Gupta, H. Narasimhan, W. Jitkrittum, A. S. Rawat, A. K. Menon, and S. Kumar. Language model cascades: Token-level uncertainty and beyond. *arXiv preprint arXiv:2404.10136*, 2024.
- [34] K. Hambardzumyan, H. Khachatrian, and J. May. Warp: Word-level adversarial reprogramming. In *Proceedings of the 59th Annual Meeting of the Association for Computational Linguistics and the 11th International Joint Conference on Natural Language Processing (Volume 1: Long Papers)*, pages 4921–4933, 2021.

- [35] L. Han, Y. Li, H. Zhang, P. Milanfar, D. Metaxas, and F. Yang. Svdiff: Compact parameter space for diffusion fine-tuning. In *Proceedings of the IEEE/CVF International Conference on Computer Vision*, pages 7323–7334, 2023.
- [36] J. He, C. Zhou, X. Ma, T. Berg-Kirkpatrick, and G. Neubig. Towards a unified view of parameter-efficient transfer learning. In *International Conference on Learning Representations*, 2021.
- [37] D. Hendrycks, C. Burns, S. Basart, A. Critch, J. Li, D. Song, and J. Steinhardt. Aligning ai with shared human values. *Proceedings of the International Conference on Learning Representations (ICLR)*, 2021.
- [38] D. Hendrycks, C. Burns, S. Basart, A. Zou, M. Mazeika, D. Song, and J. Steinhardt. Measuring massive multitask language understanding. *Proceedings of the International Conference on Learning Representations (ICLR)*, 2021.
- [39] G. E. Hinton and D. Van Camp. Keeping the neural networks simple by minimizing the description length of the weights. In *Proceedings of the sixth annual conference on Computational learning theory*, pages 5–13, 1993.
- [40] N. Houlsby, A. Giurghi, S. Jastrzebski, B. Morrone, Q. De Laroussilhe, A. Gesmundo, M. Attariyan, and S. Gelly. Parameter-efficient transfer learning for nlp. In *International conference on machine learning*, pages 2790–2799. PMLR, 2019.
- [41] E. J. Hu, Y. Shen, P. Wallis, Z. Allen-Zhu, Y. Li, S. Wang, L. Wang, and W. Chen. LoRA: Low-rank adaptation of large language models. In *International Conference on Learning Representations*, 2022.
- [42] C. Huang, R. Wang, K. Xie, T. Yu, and L. Yao. Learn when (not) to trust language models: A privacy-centric adaptive model-aware approach, 2024.
- [43] L. Huang, W. Yu, W. Ma, W. Zhong, Z. Feng, H. Wang, Q. Chen, W. Peng, X. Feng, B. Qin, and T. Liu. A survey on hallucination in large language models: Principles, taxonomy, challenges, and open questions, 2023.
- [44] S. Kadavath, T. Conerly, A. Askell, T. Henighan, D. Drain, E. Perez, N. Schiefer, Z. Hatfield-Dodds, N. DasSarma, E. Tran-Johnson, S. Johnston, S. El-Showk, A. Jones, N. Elhage, T. Hume, A. Chen, Y. Bai, S. Bowman, S. Fort, D. Ganguli, D. Hernandez, J. Jacobson, J. Kernion, S. Kravec, L. Lovitt, K. Ndousse, C. Olsson, S. Ringer, D. Amodei, T. Brown, J. Clark, N. Joseph, B. Mann, S. McCandlish, C. Olah, and J. Kaplan. Language models (mostly) know what they know, 2022.
- [45] S. Kapoor, N. Gruver, M. Roberts, K. Collins, A. Pal, U. Bhatt, A. Weller, S. Dooley, M. Goldblum, and A. G. Wilson. Large language models must be taught to know what they don’t know. *arXiv preprint arXiv:2406.08391*, 2024.
- [46] A. Kendall and Y. Gal. What uncertainties do we need in bayesian deep learning for computer vision? In I. Guyon, U. V. Luxburg, S. Bengio, H. Wallach, R. Fergus, S. Vishwanathan, and R. Garnett, editors, *Advances in Neural Information Processing Systems*, volume 30. Curran Associates, Inc., 2017.
- [47] D. P. Kingma and M. Welling. Auto-Encoding Variational Bayes. In *2nd International Conference on Learning Representations, ICLR 2014, Banff, AB, Canada, April 14-16, 2014, Conference Track Proceedings*, 2014.
- [48] R. Krishnan, P. Esposito, and M. Subedar. Bayesian-torch: Bayesian neural network layers for uncertainty estimation. <https://github.com/IntelLabs/bayesian-torch>, Jan. 2022.
- [49] R. Krishnan, M. Subedar, and O. Tickoo. Specifying weight priors in bayesian deep neural networks with empirical bayes. In *Proceedings of the AAAI Conference on Artificial Intelligence*, volume 34, pages 4477–4484, 2020.
- [50] L. Kuhn, Y. Gal, and S. Farquhar. Semantic uncertainty: Linguistic invariances for uncertainty estimation in natural language generation. *arXiv preprint arXiv:2302.09664*, 2023.

- [51] B. Lakshminarayanan, A. Pritzel, and C. Blundell. Simple and scalable predictive uncertainty estimation using deep ensembles. *Advances in neural information processing systems*, 30, 2017.
- [52] Y. LeCun. Une procedure d’apprentissage ponr reseau a seuil asymetrique. *Proceedings of Cognitiva 85*, pages 599–604, 1985.
- [53] B. Lester, R. Al-Rfou, and N. Constant. The power of scale for parameter-efficient prompt tuning. *arXiv preprint arXiv:2104.08691*, 2021.
- [54] B. Lester, R. Al-Rfou, and N. Constant. The power of scale for parameter-efficient prompt tuning. In *Proceedings of the 2021 Conference on Empirical Methods in Natural Language Processing*, pages 3045–3059, 2021.
- [55] C. Li, H. Farkhoor, R. Liu, and J. Yosinski. Measuring the intrinsic dimension of objective landscapes. *arXiv preprint arXiv:1804.08838*, 2018.
- [56] X. L. Li and P. Liang. Prefix-tuning: Optimizing continuous prompts for generation. *arXiv preprint arXiv:2101.00190*, 2021.
- [57] X. L. Li and P. Liang. Prefix-tuning: Optimizing continuous prompts for generation. In *Proceedings of the 59th Annual Meeting of the Association for Computational Linguistics and the 11th International Joint Conference on Natural Language Processing (Volume 1: Long Papers)*, pages 4582–4597, 2021.
- [58] J. Liu, Z. Lin, S. Padhy, D. Tran, T. Bedrax Weiss, and B. Lakshminarayanan. Simple and principled uncertainty estimation with deterministic deep learning via distance awareness. *Advances in neural information processing systems*, 33:7498–7512, 2020.
- [59] X. Liu, Y. Zheng, Z. Du, M. Ding, Y. Qian, Z. Yang, and J. Tang. Gpt understands, too. *AI Open*, 2023.
- [60] Y. Liu, M. Ott, N. Goyal, J. Du, M. Joshi, D. Chen, O. Levy, M. Lewis, L. Zettlemoyer, and V. Stoyanov. Roberta: A robustly optimized bert pretraining approach. *arXiv preprint arXiv:1907.11692*, 2019.
- [61] W. J. Maddox, P. Izmailov, T. Garipov, D. P. Vetrov, and A. G. Wilson. A simple baseline for bayesian uncertainty in deep learning. *Advances in neural information processing systems*, 32, 2019.
- [62] R. K. Mahabadi, S. Ruder, M. Dehghani, and J. Henderson. Parameter-efficient multi-task fine-tuning for transformers via shared hypernetworks. In *Proceedings of the 59th Annual Meeting of the Association for Computational Linguistics and the 11th International Joint Conference on Natural Language Processing (Volume 1: Long Papers)*, pages 565–576, 2021.
- [63] S. Mangrulkar, S. Gugger, L. Debut, Y. Belkada, S. Paul, and B. Bossan. Peft: State-of-the-art parameter-efficient fine-tuning methods. <https://github.com/huggingface/peft>, 2022.
- [64] T. Mihaylov, P. Clark, T. Khot, and A. Sabharwal. Can a suit of armor conduct electricity? a new dataset for open book question answering. In E. Riloff, D. Chiang, J. Hockenmaier, and J. Tsujii, editors, *Proceedings of the 2018 Conference on Empirical Methods in Natural Language Processing*, pages 2381–2391, Brussels, Belgium, Oct.-Nov. 2018. Association for Computational Linguistics.
- [65] S. Min, X. Lyu, A. Holtzman, M. Artetxe, M. Lewis, H. Hajishirzi, and L. Zettlemoyer. Rethinking the role of demonstrations: What makes in-context learning work? *arXiv preprint arXiv:2202.12837*, 2022.
- [66] R. M. Neal and G. E. Hinton. A view of the em algorithm that justifies incremental, sparse, and other variants. In *Learning in graphical models*, pages 355–368. Springer, 1998.
- [67] A. Nikitin, J. Kossen, Y. Gal, and P. Marttinen. Kernel language entropy: Fine-grained uncertainty quantification for llms from semantic similarities. *arXiv preprint arXiv:2405.20003*, 2024.

- [68] E. Onal, K. Flöge, E. Caldwell, A. Sheverdin, and V. Fortuin. Gaussian stochastic weight averaging for bayesian low-rank adaptation of large language models, 2024.
- [69] V. M.-H. Ong, D. J. Nott, and M. S. Smith. Gaussian variational approximation with a factor covariance structure. *Journal of Computational and Graphical Statistics*, 27(3):465–478, 2018.
- [70] OpenAI. Introducing chatgpt. [online]. available: <https://openai.com/blog/chatgpt>. 2022.
- [71] M. Opper and C. Archambeau. The variational gaussian approximation revisited. *Neural computation*, 21(3):786–792, 2009.
- [72] Y. Park and D. Blei. Density uncertainty layers for reliable uncertainty estimation. In *International Conference on Artificial Intelligence and Statistics*, pages 163–171. PMLR, 2024.
- [73] E. Parzen. On Estimation of a Probability Density Function and Mode. *The Annals of Mathematical Statistics*, 33(3):1065 – 1076, 1962.
- [74] J. Pfeiffer, A. Kamath, A. Rücklé, K. Cho, and I. Gurevych. Adapterfusion: Non-destructive task composition for transfer learning. In *Proceedings of the 16th Conference of the European Chapter of the Association for Computational Linguistics: Main Volume*, pages 487–503, 2021.
- [75] M. T. Pilehvar and J. Camacho-Collados. WiC: the word-in-context dataset for evaluating context-sensitive meaning representations. In J. Burstein, C. Doran, and T. Solorio, editors, *Proceedings of the 2019 Conference of the North American Chapter of the Association for Computational Linguistics: Human Language Technologies, Volume 1 (Long and Short Papers)*, pages 1267–1273, Minneapolis, Minnesota, June 2019. Association for Computational Linguistics.
- [76] A. Radford, J. Wu, R. Child, D. Luan, D. Amodei, I. Sutskever, et al. Language models are unsupervised multitask learners. *OpenAI blog*, 1(8):9, 2019.
- [77] D. J. Rezende, S. Mohamed, and D. Wierstra. Stochastic backpropagation and approximate inference in deep generative models. In *International conference on machine learning*, pages 1278–1286. PMLR, 2014.
- [78] M. Rosenblatt. Remarks on Some Nonparametric Estimates of a Density Function. *The Annals of Mathematical Statistics*, 27(3):832 – 837, 1956.
- [79] A. Rücklé, G. Geigle, M. Glockner, T. Beck, J. Pfeiffer, N. Reimers, and I. Gurevych. Adapterdrop: On the efficiency of adapters in transformers. In *Proceedings of the 2021 Conference on Empirical Methods in Natural Language Processing*, pages 7930–7946, 2021.
- [80] D. E. Rumelhart, G. E. Hinton, and R. J. Williams. Learning representations by back-propagating errors. *nature*, 323(6088):533–536, 1986.
- [81] K. Sakaguchi, R. L. Bras, C. Bhagavatula, and Y. Choi. Winogrande: an adversarial winograd schema challenge at scale. *Commun. ACM*, 64(9):99–106, aug 2021.
- [82] H. Shi, Z. Xu, H. Wang, W. Qin, W. Wang, Y. Wang, and H. Wang. Continual learning of large language models: A comprehensive survey, 2024.
- [83] L. S. Tan and D. J. Nott. Gaussian variational approximation with sparse precision matrices. *Statistics and Computing*, 28:259–275, 2018.
- [84] K. Tian, E. Mitchell, A. Zhou, A. Sharma, R. Rafailov, H. Yao, C. Finn, and C. Manning. Just ask for calibration: Strategies for eliciting calibrated confidence scores from language models fine-tuned with human feedback. In H. Bouamor, J. Pino, and K. Bali, editors, *Proceedings of the 2023 Conference on Empirical Methods in Natural Language Processing*, pages 5433–5442, Singapore, Dec. 2023. Association for Computational Linguistics.

- [85] L. Tierney and J. B. Kadane. Accurate approximations for posterior moments and marginal densities. *Journal of the american statistical association*, 81(393):82–86, 1986.
- [86] M. Titsias and M. Lázaro-Gredilla. Doubly stochastic variational bayes for non-conjugate inference. In E. P. Xing and T. Jebara, editors, *Proceedings of the 31st International Conference on Machine Learning*, volume 32 of *Proceedings of Machine Learning Research*, pages 1971–1979, Beijing, China, 22–24 Jun 2014. PMLR.
- [87] M. Tomczak, S. Swaroop, and R. Turner. Efficient low rank gaussian variational inference for neural networks. *Advances in Neural Information Processing Systems*, 33:4610–4622, 2020.
- [88] H. Touvron, T. Lavril, G. Izacard, X. Martinet, M.-A. Lachaux, T. Lacroix, B. Rozière, N. Goyal, E. Hambro, F. Azhar, et al. Llama: Open and efficient foundation language models. *arXiv preprint arXiv:2302.13971*, 2023.
- [89] H. Touvron, L. Martin, K. Stone, P. Albert, A. Almahairi, Y. Babaei, N. Bashlykov, S. Batra, P. Bhargava, S. Bhosale, et al. Llama 2: Open foundation and fine-tuned chat models. *arXiv preprint arXiv:2307.09288*, 2023.
- [90] D. Tran, M. Dusenberry, M. Van Der Wilk, and D. Hafner. Bayesian layers: A module for neural network uncertainty. *Advances in neural information processing systems*, 32, 2019.
- [91] T. Vu, B. Lester, N. Constant, R. Al-Rfou, and D. Cer. Spot: Better frozen model adaptation through soft prompt transfer. In *Proceedings of the 60th Annual Meeting of the Association for Computational Linguistics (Volume 1: Long Papers)*, pages 5039–5059, 2022.
- [92] A. Wang, Y. Pruksachatkun, N. Nangia, A. Singh, J. Michael, F. Hill, O. Levy, and S. R. Bowman. *SuperGLUE: a stickier benchmark for general-purpose language understanding systems*. Curran Associates Inc., Red Hook, NY, USA, 2019.
- [93] A. Wang, A. Singh, J. Michael, F. Hill, O. Levy, and S. Bowman. GLUE: A multi-task benchmark and analysis platform for natural language understanding. In T. Linzen, G. Chrupala, and A. Alishahi, editors, *Proceedings of the 2018 EMNLP Workshop BlackboxNLP: Analyzing and Interpreting Neural Networks for NLP*, pages 353–355, Brussels, Belgium, Nov. 2018. Association for Computational Linguistics.
- [94] H. Wang, X. Shi, and D.-Y. Yeung. Natural-parameter networks: A class of probabilistic neural networks. *Advances in neural information processing systems*, 29, 2016.
- [95] H. Wang and D.-Y. Yeung. A survey on bayesian deep learning. *ACM computing surveys (csur)*, 53(5):1–37, 2020.
- [96] X. Wang, L. Aitchison, and M. Rudolph. Lora ensembles for large language model fine-tuning, 2023.
- [97] A. Warstadt, A. Singh, and S. R. Bowman. Neural network acceptability judgments. *Transactions of the Association for Computational Linguistics*, 7:625–641, 2019.
- [98] J. Wei, M. Bosma, V. Y. Zhao, K. Guu, A. W. Yu, B. Lester, N. Du, A. M. Dai, and Q. V. Le. Finetuned language models are zero-shot learners. *arXiv preprint arXiv:2109.01652*, 2021.
- [99] J. Wei, Y. Tay, R. Bommasani, C. Raffel, B. Zoph, S. Borgeaud, D. Yogatama, M. Bosma, D. Zhou, D. Metzler, et al. Emergent abilities of large language models. *arXiv preprint arXiv:2206.07682*, 2022.
- [100] L. Weidinger, J. Mellor, M. Rauh, C. Griffin, J. Uesato, P.-S. Huang, M. Cheng, M. Glaese, B. Balle, A. Kasirzadeh, Z. Kenton, S. Brown, W. Hawkins, T. Stepleton, C. Biles, A. Birhane, J. Haas, L. Rimell, L. A. Hendricks, W. Isaac, S. Legassick, G. Irving, and I. Gabriel. Ethical and social risks of harm from language models, 2021.
- [101] Y. Wen, P. Vicol, J. Ba, D. Tran, and R. Grosse. Flipout: Efficient pseudo-independent weight perturbations on mini-batches. In *International Conference on Learning Representations*, 2018.

- [102] J. G. Wiese, L. Wimmer, T. Papamarkou, B. Bischl, S. Günnemann, and D. Rügamer. Towards efficient mcmc sampling in bayesian neural networks by exploiting symmetry. In *Joint European Conference on Machine Learning and Knowledge Discovery in Databases*, pages 459–474. Springer, 2023.
- [103] A. G. Wilson and P. Izmailov. Bayesian deep learning and a probabilistic perspective of generalization, 2022.
- [104] M. Xiong, Z. Hu, X. Lu, Y. Li, J. Fu, J. He, and B. Hooi. Can llms express their uncertainty? an empirical evaluation of confidence elicitation in llms. *arXiv preprint arXiv:2306.13063*, 2023.
- [105] R. Xu, F. Luo, Z. Zhang, C. Tan, B. Chang, S. Huang, and F. Huang. Raise a child in large language model: Towards effective and generalizable fine-tuning. In *Proceedings of the 2021 Conference on Empirical Methods in Natural Language Processing*, pages 9514–9528, 2021.
- [106] B. Xue, J. Yu, J. Xu, S. Liu, S. Hu, Z. Ye, M. Geng, X. Liu, and H. Meng. Bayesian transformer language models for speech recognition. In *ICASSP 2021-2021 IEEE International Conference on Acoustics, Speech and Signal Processing (ICASSP)*, pages 7378–7382. IEEE, 2021.
- [107] Y. A. Yadkori, I. Kuzborskij, A. György, and C. Szepesvári. To believe or not to believe your llm. *arXiv preprint arXiv:2406.02543*, 2024.
- [108] A. X. Yang, M. Robeyns, X. Wang, and L. Aitchison. Bayesian low-rank adaptation for large language models. *arXiv preprint arXiv:2308.13111*, 2023.
- [109] J. S. Yedidia, W. Freeman, and Y. Weiss. Generalized belief propagation. *Advances in neural information processing systems*, 13, 2000.
- [110] Z. Yin, Q. Sun, Q. Guo, J. Wu, X. Qiu, and X. Huang. Do large language models know what they don’t know? *arXiv preprint arXiv:2305.18153*, 2023.
- [111] E. B. Zaken, Y. Goldberg, and S. Ravfogel. Bitfit: Simple parameter-efficient fine-tuning for transformer-based masked language-models. In *Proceedings of the 60th Annual Meeting of the Association for Computational Linguistics (Volume 2: Short Papers)*, pages 1–9, 2022.
- [112] H. Zhang, S. Diao, Y. Lin, Y. R. Fung, Q. Lian, X. Wang, Y. Chen, H. Ji, and T. Zhang. R-tuning: Teaching large language models to refuse unknown questions. *arXiv preprint arXiv:2311.09677*, 2023.
- [113] J. O. Zhang, A. Sax, A. Zamir, L. Guibas, and J. Malik. Side-tuning: a baseline for network adaptation via additive side networks. In *Computer Vision–ECCV 2020: 16th European Conference, Glasgow, UK, August 23–28, 2020, Proceedings, Part III 16*, pages 698–714. Springer, 2020.
- [114] R. Zhang, C. Li, J. Zhang, C. Chen, and A. G. Wilson. Cyclical stochastic gradient mcmc for bayesian deep learning. *arXiv preprint arXiv:1902.03932*, 2019.
- [115] S. Zhang, X. Fan, B. Chen, and M. Zhou. Bayesian attention belief networks. In *International Conference on Machine Learning*, pages 12413–12426. PMLR, 2021.
- [116] M. Zhao, T. Lin, F. Mi, M. Jaggi, and H. Schütze. Masking as an efficient alternative to finetuning for pretrained language models. In *Proceedings of the 2020 Conference on Empirical Methods in Natural Language Processing (EMNLP)*, pages 2226–2241, 2020.

Appendix

In Appendix A, we present the proofs for the theorems in the main body of our paper. In Appendix B, we introduce the experimental settings, including evaluation metrics and training schemes. Finally, in Appendix C, we present supplementary empirical results including the experiments on another language model and analysis of the space and time cost of our algorithm.

A Proof of Theorems and Claims

In this section, we first present the proof of the two main theorems (Theorem 3.1 and Theorem 3.2) in Appendix A.1. Next, we show how a analysis on our design of parameterization in Appendix A.2. Finally, we provide a detailed derivation of the LoRA Flipout in Appendix A.3.

A.1 Proof of Main Theorems

Theorem 3.1 (Variational Distribution of the Full-Weight Matrix in BLoB). *With the pre-trained weight matrix $\mathbf{W}_0 \in \mathbb{R}^{m \times n}$ and the low-rank weight update matrix $\mathbf{B} \in \mathbb{R}^{m \times r}$, suppose that the variational distribution of the other low-rank update matrix $\mathbf{A} \in \mathbb{R}^{r \times n}$ is Gaussian with $q(\mathbf{A}|\boldsymbol{\theta} = \{\mathbf{M}, \boldsymbol{\Omega}\}) = \prod_{ij} \mathcal{N}(A_{ij}|M_{ij}, \Omega_{ij}^2)$, where $\mathbf{M} = [M_{ij}] \in \mathbb{R}^{r \times n}$ and $\boldsymbol{\Omega} = [\Omega_{ij}] \in \mathbb{R}^{r \times n}$ are its mean and standard deviation, respectively. The equivalent variational distribution defined on the full weight matrix \mathbf{W} as in Eqn. 3 is given by*

$$\begin{aligned} q(\text{vec}(\mathbf{W})|\mathbf{B}, \boldsymbol{\theta}) &= \mathcal{N}(\text{vec}(\mathbf{W})|\boldsymbol{\mu}_q, \boldsymbol{\Sigma}_q), \\ \text{where } \boldsymbol{\mu}_q &= \text{vec}(\mathbf{W}_0 + \mathbf{B}\mathbf{M}), \\ \boldsymbol{\Sigma}_q &= [\mathbf{I}_n \otimes \mathbf{B}] \cdot [\text{diag}(\text{vec}(\boldsymbol{\Omega}^2))] \cdot [\mathbf{I}_n \otimes \mathbf{B}^\top]. \end{aligned}$$

Proof. We begin by calculating the mean value of q ,

$$\boldsymbol{\mu}_q = \text{vec}(\mathbb{E}[\mathbf{W}_0 + \mathbf{B}\mathbf{A}]) \quad (14)$$

$$= \text{vec}(\mathbf{W}_0 + \mathbf{B}\mathbb{E}[\mathbf{A}]) \quad (15)$$

$$= \text{vec}(\mathbf{W}_0 + \mathbf{B}\mathbf{M}). \quad (16)$$

Suppose the deterministic matrix $\mathbf{B} = [\mathbf{b}_1, \mathbf{b}_2, \dots, \mathbf{b}_r] \in \mathbb{R}^{m \times r}$, random matrix $\mathbf{A} = [\mathbf{a}_1, \mathbf{a}_2, \dots, \mathbf{a}_r]^\top \in \mathbb{R}^{r \times n}$, with its underlying parameters of mean and standard deviation defined likewise $\mathbf{M} \in \mathbb{R}^{r \times n}$ and $\boldsymbol{\Omega} \in \mathbb{R}^{r \times n}$. We have $\mathbf{W} = \mathbf{B}\mathbf{A} = \sum_{i=1}^r \mathbf{b}_i \cdot \mathbf{a}_i^\top$. We then rewrite $\text{vec}(\mathbf{W})$ in the form of Kronecker product \otimes :

$$\text{vec}(\mathbf{W}) = \text{vec}\left(\sum_{i=1}^r \mathbf{b}_i \cdot \mathbf{a}_i^\top\right) = \sum_{i=1}^r (\mathbf{a}_i \otimes \mathbf{b}_i) \quad (17)$$

We then calculate the covariance matrix $\boldsymbol{\Sigma}_q$ as

$$\boldsymbol{\Sigma}_q = \text{cov}[\text{vec}(\mathbf{W}), \text{vec}(\mathbf{W})] = \text{cov}\left[\sum_{i=1}^r (\mathbf{a}_i \otimes \mathbf{b}_i), \sum_{i=1}^r (\mathbf{a}_i \otimes \mathbf{b}_i)\right] \quad (18)$$

$$= \sum_{i=1}^r \text{cov}[\mathbf{a}_i \otimes \mathbf{b}_i, \mathbf{a}_i \otimes \mathbf{b}_i] + \sum_{i \neq j} \text{cov}[\mathbf{a}_i \otimes \mathbf{b}_i, \mathbf{a}_j \otimes \mathbf{b}_j] \quad (19)$$

$$= \sum_{i=1}^r \mathbb{E}_{\mathbf{a}_i}[(\mathbf{a}_i \otimes \mathbf{b}_i)(\mathbf{a}_i \otimes \mathbf{b}_i)^\top] \quad (20)$$

$$= \sum_{i=1}^r \mathbb{E}_{\mathbf{a}_i}[(\mathbf{a}_i \mathbf{a}_i^\top) \otimes (\mathbf{b}_i \mathbf{b}_i^\top)] = \sum_{i=1}^r \mathbb{E}_{\mathbf{a}_i}[(\mathbf{a}_i \mathbf{a}_i^\top)] \otimes (\mathbf{b}_i \mathbf{b}_i^\top) \quad (21)$$

$$= \sum_{i=1}^r \text{diag}(\boldsymbol{\sigma}_i^2) \otimes (\mathbf{b}_i \mathbf{b}_i^\top) \quad (22)$$

$$= [\mathbf{I}_n \otimes \mathbf{B}] \cdot [\text{diag}(\text{vec}(\boldsymbol{\Omega}^2))] \cdot [\mathbf{I}_n \otimes \mathbf{B}^\top], \quad (23)$$

completing the proof. \square

It is crucial to note here, the final covariance matrix of $q(\text{vec}(\mathbf{W}))$ follows a block-diagonal structure, which will be further utilized for the proof of Theorem 3.2. Defining $\Sigma_i = \text{diag}(\Omega_{i:}^2)$, we have:

$$\Sigma_q = \begin{bmatrix} \mathbf{B}\Sigma_1\mathbf{B}^\top & & & \\ & \ddots & & \\ & & \ddots & \\ & & & \mathbf{B}\Sigma_n\mathbf{B}^\top \end{bmatrix}. \quad (24)$$

Another important fact about Σ_q is its singularity. It can be seen directly as we consider the rank of any one of the block matrix $\mathbf{B}\Sigma_i\mathbf{B}^\top \in \mathbb{R}^{m \times m}, \forall i \in [n]$:

$$r(\mathbf{B}\Sigma\mathbf{B}^\top) \leq \min\{r(\mathbf{B}), r(\Sigma_i), r(\mathbf{B}^\top)\} \leq r < m, \quad (25)$$

where r is the rank of LoRA, strictly smaller than the output dimension of m .

Theorem 3.2 (Efficient Computation of Full-Weight KL Divergence). *Suppose the pre-trained weights \mathbf{W}_0 , update matrix \mathbf{B} , and the variational distribution $q(\mathbf{A}|\theta)$ are defined as in Theorem 3.1, and the prior distribution of the full-weight matrix $P(\text{vec}(\mathbf{W}))$ is defined as Eqn. 9. Consider the Gaussian prior distribution $P(\mathbf{A}) = \prod_{ij} \mathcal{N}(A_{ij}|0, \sigma_p^2)$; we then have:*

$$\text{KL}[q(\text{vec}(\mathbf{W})|\mathbf{B}, \theta) \| P(\text{vec}(\mathbf{W}))] = \text{KL}[q(\mathbf{A}|\theta) \| P(\mathbf{A})],$$

if $\tilde{\mathbf{R}} = [\sigma_p \mathbf{I}_n \otimes \mathbf{R}]$, where \mathbf{R} satisfies $\mathbf{R}\mathbf{R}^\top = \mathbf{B}\mathbf{B}^\top$.

Proof. We start by assuming the low-rank structure of the prior $P(\text{vec}(\mathbf{W}))$, and then reveal the conditions reaching to our final conclusion step by step.

Typically, for two Gaussian distributions q and p whose covariance matrices $\Sigma_q \in \mathbb{R}^{d \times d}$ and $\Sigma_p \in \mathbb{R}^{d \times d}$ are both full-rank, and their means as $\mu_q \in \mathbb{R}^d$ and $\mu_p \in \mathbb{R}^d$, we have their KL-divergence as

$$\text{KL}[q \| p] = \frac{1}{2} \left[\log \frac{|\Sigma_p|}{|\Sigma_q|} - d + \text{tr}(\Sigma_p^{-1}\Sigma_q) + (\mu_q - \mu_p)^\top \Sigma_p^{-1}(\mu_q - \mu_p) \right]. \quad (26)$$

The singularity of the covariance matrices of $P(\text{vec}(\mathbf{W}))$ and $q(\text{vec}(\mathbf{W}))$, i.e., $|\Sigma_q| = |\Sigma_p| = 0$, can cause issues when computing the KL-divergence as it includes the log-determinant term. Therefore in this proof, we consider the alternative of the covariance matrices, where an extremely small diagonal elements are added.

For the prior distribution, as suggested in Eqn. 9, we assume

$$P(\text{vec}(\mathbf{W})) = \mathcal{N}(\mathbf{W}_0, \Sigma_p), \quad (27)$$

$$\text{where } \Sigma_p = \lambda \mathbf{I} + \tilde{\mathbf{R}}\tilde{\mathbf{R}}^\top, \quad (\lambda \rightarrow 0^+).$$

By default, we assume that the low-rank tall matrix $\tilde{\mathbf{R}} \in \mathbb{R}^{(mn) \times r'}$ has the full column rank r' . Otherwise if $r(\tilde{\mathbf{R}}) = r'' < r'$, then we can in effect consider a new matrix component $\tilde{\mathbf{R}}' \in \mathbb{R}^{(mn) \times r''}$ that has the same rank as r'' , which satisfies our assumption of full column rank. Therefore, we assume that the result of the SVD decomposition of $\tilde{\mathbf{R}}$ is given by

$$\tilde{\mathbf{R}} = \mathbf{U}_R \mathbf{D}_R \mathbf{V}_R^\top, \quad (28)$$

where $\mathbf{U}_R \in \mathbb{R}^{(mn) \times (mn)}$ and $\mathbf{V}_R \in \mathbb{R}^{r' \times r'}$ are orthogonal, i.e., $\mathbf{U}_R \mathbf{U}_R^\top = \mathbf{U}_R^\top \mathbf{U}_R = \mathbf{I}_{(mn)}$ and $\mathbf{V}_R \mathbf{V}_R^\top = \mathbf{V}_R^\top \mathbf{V}_R = \mathbf{I}_{r'}$. \mathbf{D}_R is a tall matrix where its upper part is diagonal and the lower part is a zero matrix, denoted as $\mathbf{D}_R = [\mathbf{D}_R^*, \mathbf{O}]^\top = [\text{diag}([d_{R_1} > 0, d_{R_2} > 0, \dots, d_{R_{r'}} > 0]), \mathbf{O}]^\top$.

For the approximate posterior $q(\text{vec}(\mathbf{W})|\mathbf{B}, \theta)$, we consider

$$q(\text{vec}(\mathbf{W})|\mathbf{B}, \theta) = \mathcal{N}(\mathbf{W}_0 + \mathbf{B}\mathbf{M}, \Sigma_q), \quad (29)$$

$$\text{where } \Sigma_q = \lambda \mathbf{I} + \tilde{\mathbf{B}}\Sigma\tilde{\mathbf{B}}^\top, \quad (\lambda \rightarrow 0^+),$$

where we simplify the notation for the covariance matrix Σ_q by defining $\tilde{\mathbf{B}} = [\mathbf{I}_n \otimes \mathbf{B}] \in \mathbb{R}^{(mn) \times (mr)}$ and $\Sigma = \text{diag}(\text{vec}(\Omega)^2)$. Likewise, we have the SVD-decomposed matrices for $\tilde{\mathbf{B}}$ where they are defined in the same way as Eqn. 28:

$$\tilde{\mathbf{B}} = \mathbf{U}_B \mathbf{D}_B \mathbf{V}_B^\top, \quad (30)$$

where \mathbf{U}_B and \mathbf{V}_B are orthogonal matrices, and $\mathbf{D}_B = [\mathbf{D}_B^*, \mathbf{O}]^\top = [\text{diag}([d_{B_1} > 0, d_{B_2} > 0, \dots, d_{B_{mr}} > 0]), \mathbf{O}]^\top$.

First, we calculate the log-determinant part of the KL-divergence. For the log-determinant of the covariance matrix of the prior distribution Σ_p , by applying SVD decomposition in Eqn. 28, we have

$$\log |\Sigma_p| = \log |\lambda \mathbf{I} + \tilde{\mathbf{R}}\tilde{\mathbf{R}}^\top| = \log |\lambda \mathbf{I} + \mathbf{U}_R \mathbf{D}_R \mathbf{V}_R^\top \mathbf{V}_R \mathbf{D}_R^\top \mathbf{U}_R^\top| \quad (31)$$

$$= \log |\mathbf{U}_R (\lambda \mathbf{I} + \mathbf{D}_R \mathbf{D}_R^\top) \mathbf{U}_R^\top| \quad (32)$$

$$= \log \left| \mathbf{U}_R \begin{bmatrix} (\mathbf{D}_R^*)^2 + \lambda \mathbf{I}_{r'} & \mathbf{O} \\ \mathbf{O} & \lambda \mathbf{I}_{mn-r'} \end{bmatrix} \mathbf{U}_R^\top \right| \quad (33)$$

$$= \log |(\mathbf{D}_R^*)^2 + \lambda \mathbf{I}_{r'}| + \log |\lambda \mathbf{I}_{mn-r'}| \quad (34)$$

$$= (mn - r') \log \lambda + \sum_{i=1}^{r'} \log (d_{R_i}^2 + \lambda). \quad (35)$$

Following (almost) the same idea, we now have the log-determinant of the variational distribution's covariance Σ_q as

$$\log |\Sigma_q| = \log |\lambda \mathbf{I} + \tilde{\mathbf{B}}\tilde{\mathbf{B}}^\top| = \log \left| \begin{bmatrix} \mathbf{D}_B^* \mathbf{V}_B^\top \Sigma \mathbf{V}_B \mathbf{D}_B^* + \lambda \mathbf{I}_{mr} & \mathbf{O} \\ \mathbf{O} & \lambda \mathbf{I}_{mn-mr} \end{bmatrix} \right| \quad (36)$$

$$= (mn - mr) \log \lambda + 2 \log |\mathbf{D}_B^*| + \log |\mathbf{V}_B^\top \Sigma \mathbf{V}_B + \lambda (\mathbf{D}_B^*)^{-2}| \quad (37)$$

$$= (mn - mr) \log \lambda + 2 \sum_{i=1}^{mr} \log d_{B_i} + \log |\Sigma| + \log |\mathbf{I} + \lambda \mathbf{V}_B^\top \Sigma^{-1} \mathbf{V}_B (\mathbf{D}_B^*)^{-2}|. \quad (38)$$

We make two observations when $\lambda \rightarrow 0^+$: (i) compare the terms that contain $\log \lambda$ on both sides, to make sure the log-determinant in the divergence term *bounded*, we have to set $r' = mr$; (ii) the last term in Eqn. 38, $\log |\mathbf{I} + \lambda \mathbf{V}_B^\top \Sigma^{-1} \mathbf{V}_B (\mathbf{D}_B^*)^{-2}| = \log |\mathbf{I}| = 0$. Therefore, we have

$$\log \frac{|\Sigma_p|}{|\Sigma_q|} = \sum_{i=1}^{mr} \log \frac{d_{R_i}^2 + \lambda}{d_{B_i}^2} - \log |\Sigma|. \quad (39)$$

Next we calculate $\text{tr}(\Sigma_p^{-1} \Sigma_q)$ in Eqn. 26. Following the same assumptions and notations above, we have the inverse of the covariance of the prior distribution as

$$\Sigma_p^{-1} = \mathbf{U}_R \begin{bmatrix} [(\mathbf{D}_R^*)^2 + \lambda \mathbf{I}]^{-1} & \mathbf{O} \\ \mathbf{O} & \lambda^{-1} \mathbf{I} \end{bmatrix} \mathbf{U}_R^\top. \quad (40)$$

Hence we have

$$\text{tr}(\Sigma_p^{-1} \Sigma_q) = \text{tr}(\mathbf{U}_R \begin{bmatrix} [(\mathbf{D}_R^*)^2 + \lambda \mathbf{I}]^{-1} & \mathbf{O} \\ \mathbf{O} & \lambda^{-1} \mathbf{I} \end{bmatrix} \mathbf{U}_R^\top \mathbf{U}_B \begin{bmatrix} \mathbf{D}_B^* \mathbf{V}_B^\top \Sigma \mathbf{V}_B \mathbf{D}_B^* + \lambda \mathbf{I} & \mathbf{O} \\ \mathbf{O} & \lambda \mathbf{I} \end{bmatrix} \mathbf{U}_B^\top). \quad (41)$$

By using the condition $\mathbf{R}\mathbf{R}^\top = \mathbf{B}\mathbf{B}^\top$ and $\tilde{\mathbf{R}} = [\sigma_p \mathbf{I}_n \otimes \mathbf{R}]$ defined in Theorem 3.2, we have

$$\tilde{\mathbf{R}}\tilde{\mathbf{R}}^\top = \sigma_p^2 \tilde{\mathbf{B}}\tilde{\mathbf{B}}^\top, \quad (42)$$

and there exists an orthogonal matrix $\mathbf{P} \in \mathbb{R}^{(mr) \times (mr)}$, such that

$$\tilde{\mathbf{R}} = \sigma_p \tilde{\mathbf{B}} \mathbf{P}. \quad (43)$$

The SVD decomposition on $\tilde{\mathbf{R}}$ can then be formulated as:

$$\tilde{\mathbf{R}} = \sigma_p \mathbf{U}_B \mathbf{D}_B \mathbf{V}_B^\top \mathbf{P} \quad (44)$$

$$= (\mathbf{U}_R = \mathbf{U}_B) (\mathbf{D}_R = \sigma_p \mathbf{D}_B) (\mathbf{V}_R = \mathbf{V}_B^\top \mathbf{P}). \quad (45)$$

Substituting $\mathbf{U}_R, \mathbf{D}_R, \mathbf{V}_R$ back to Eqn. 41 and applying $\lambda \rightarrow 0^+$, we have

$$\text{tr}(\Sigma_p^{-1} \Sigma_q) = \text{tr}(\mathbf{I}_{mn-nr}) + \text{tr}([\sigma_p \mathbf{D}^*]^2 + \lambda \mathbf{I})^{-1} [\mathbf{D}_B^* \mathbf{V}_B^\top \Sigma \mathbf{V}_B \mathbf{D}_B^*] \quad (46)$$

$$= (mn - nr) + \sigma_p^{-2} \text{tr}(\mathbf{V}_B^\top \Sigma \mathbf{V}_B) \quad (47)$$

$$= (mn - nr) + \sigma_p^{-2} \text{tr}(\Sigma). \quad (48)$$

For the quadratic term in Eqn. 26, the pre-trained weights \mathbf{W}_0 cancel out, and we can calculate it as

$$\text{vec}(\mathbf{B}\mathbf{M})^\top \boldsymbol{\Sigma}_p^{-1} \text{vec}(\mathbf{B}\mathbf{M}) \quad (49)$$

$$= [\mathbf{M}_{:1}^\top \mathbf{B}^\top, \dots, \mathbf{M}_{:1}^\top \mathbf{B}^\top] \begin{bmatrix} (\mathbf{B}\boldsymbol{\Sigma}_1 \mathbf{B}^\top)^{-1} & & \\ & \ddots & \\ & & (\mathbf{B}\boldsymbol{\Sigma}_n \mathbf{B}^\top)^{-1} \end{bmatrix} \begin{bmatrix} \mathbf{B}\mathbf{M}_{:1} \\ \vdots \\ \mathbf{B}\mathbf{M}_{:n} \end{bmatrix} \quad (50)$$

$$= \sum_{i=1}^n \mathbf{M}_{:i}^\top \mathbf{B}^\top (\mathbf{B}\boldsymbol{\Sigma}_i \mathbf{B}^\top)^{-1} \mathbf{B}\mathbf{M}_{:i} \quad (51)$$

$$= \sum_{i=1}^n \mathbf{M}_{:i}^\top (\mathbf{V}_B \begin{bmatrix} \frac{d_{B_1}^2}{\sigma_p^2(d_{B_1}^2 + \lambda)} & & \\ & \ddots & \\ & & \frac{d_{B_{mr}}^2}{\sigma_p^2(d_{B_{mr}}^2 + \lambda)} \end{bmatrix} \mathbf{V}_B^\top) \mathbf{M}_{:i} \quad (52)$$

$$= \frac{1}{\sigma_p^2} \sum_{i=1}^n \mathbf{M}_{:i}^\top \mathbf{M}_{:i} \quad (53)$$

$$= \frac{1}{\sigma_p^2} \|\mathbf{M}\|_2^2. \quad (54)$$

Finally, proof is completed by combining Eqn. 39, Eqn. 48, and Eqn. 54. \square

A.2 Analysis on BLoB Parameterization

General Analysis on Parameterization. Consider a path of parameterization for a single variable:

$$\rho \rightarrow \sigma = f(\rho) \rightarrow \mathcal{L} = l(\sigma), \quad (55)$$

where ρ is the real parameter we perform update on, f is our parameterization choice for the variable σ , and l represents the loss function we aim to minimize. When comparing two different parameterization methods, we consider the same initial conditions of $\sigma = \sigma_0$, and we assume the same step size η on the real parameter ρ . To show the influence of the choice of parameterization, we calculate the decrease of the loss value by performing one step of gradient descent. First, by the chain rule, the gradient w.r.t. ρ_0 is calculated as

$$\frac{d\mathcal{L}}{d\rho} \Big|_{\rho_0} = \frac{d\mathcal{L}}{d\sigma} \Big|_{\sigma_0} \cdot \frac{d\sigma}{d\rho} \Big|_{\rho_0} = l'(\sigma_0) \cdot f'(\rho_0). \quad (56)$$

After one step of the gradient descent, we have ρ_1 as

$$\rho_1 = \rho_0 - \eta \cdot l'(\sigma_0) \cdot f'(\rho_0), \quad (57)$$

and the loss value decreased at ρ_1 can be approximated by the first-order Taylor expansion,

$$\Delta\mathcal{L} = l(f(\rho_0)) - l(f(\rho_1)) \quad (58)$$

$$= l(f(\rho_0)) - [l(f(\rho_0 - \eta \cdot l'(\sigma_0) \cdot f'(\rho_0)))] \quad (59)$$

$$\approx l(f(\rho_0)) - [l(f(\rho_0) - \eta \cdot l'(\sigma_0) \cdot (f'(\rho_0))^2)] \quad (60)$$

$$\approx \eta \cdot (l'(\sigma_0))^2 \cdot (f'(\rho_0))^2. \quad (61)$$

Since the initialization of the different parameterization variable ρ_0 is set to ensure the same initial condition of σ_0 for different f s, we can see that the amount the loss decreases by after one step of update is proportional to the squared gradient $\Delta\mathcal{L} \propto (l'(\sigma_0))^2 \cdot (f'(\rho))^2 = (d\mathcal{L}/d\rho)^2$.

Parameterization with $\log(1 + \exp(\cdot))$ or $(\cdot)^2$? Previous VBNS [11, 49] typically use a softplus function $\sigma_q = \log(1 + \exp(\rho))$ to parameterize the standard deviation. For a single element ρ , the derivative of the closed-form solution of the KL divergence in Eqn. 11 is calculated as

$$\frac{d\text{KL}}{d\rho} = -\frac{e^\rho}{(1+e^\rho)\log(1+e^\rho)} + \frac{e^\rho \log(1+e^\rho)}{\sigma_p^2(1+e^\rho)}. \quad (62)$$

Due to the fact that σ_q is typically initialized to a small value close to 0 to ensure stable optimization of the likelihood cost term (e.g., $1e-3$), and in order to ensure that the model obtains good uncertainty,

σ_p is usually set to a larger value close to 1 (e.g., $1e-1$). In this case, the derivative of ρ in Eqn. 62 is almost always a constant -1 , which, based on our previous analysis, leads to slow convergence for large σ_p values when σ_q is small.

Therefore, we parameterize σ_q with quadratic function: $\sigma_q = \rho^2$. In this case, the derivative of the KL divergence with respect to ρ in Eqn. 11 becomes:

$$\frac{d\text{KL}}{d\rho} = -\frac{2}{\rho} + \frac{2\rho^3}{\sigma_p^2}. \quad (63)$$

Under the same initialization conditions, the derivative in Eqn. 63 is approximately of the order of ρ^{-1} , leading to rapid convergence towards larger σ_p values when σ_q is small. Building on this, we use SGD without momentum to optimize the complexity loss term, thereby achieving the natural convergence of σ_q .

Visual Demonstration. To visually demonstrate the differences in the convergence of KL divergence during training with these two parameterizations, we set $\sigma_p = 1$ and employ gradient descent to optimize the KL divergence. As introduced in B.1, in practical mini-batch gradient descent, the KL divergence is weighted by $1/\#\text{mini-batches}$. Therefore, assuming there are 100 mini-batches, the learning rate is set to 0.01, which translates to an actual learning rate of $1e-4$ for ρ . We initialize $\sigma_q = 0.01$ for both parameterizations. The growth of σ_q during the KL training, for $\sigma_q = \log(1 + e^\rho)$ and $\sigma_q = \rho^2$ is shown in Fig. 2. In the same setting, the softplus parameterization takes nearly 100,000 iterations to converge, while the square parameterization takes only about 5,000 iterations.

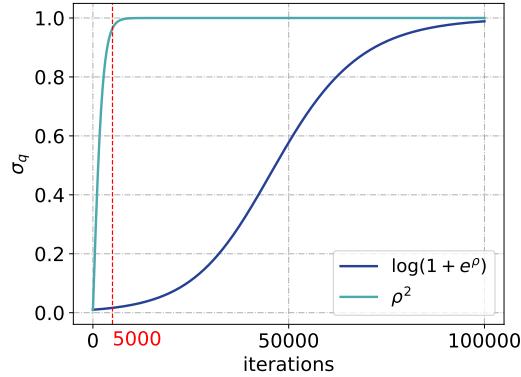


Figure 2: The growth curve of $\sigma_q = \log(1 + e^\rho)$ and $\sigma_q = \rho^2$ during the optimization of KL divergence (without data likelihood). The number of training steps (5000) is marked with the red line.

A.3 Deriving Flipout for BLoB

For the i -th input vector \mathbf{h}_i in a mini-batch, we randomly sample two flipping vector $\mathbf{s} \in \{-1, +1\}^n$ and $\mathbf{t} \in \{-1, +1\}^r$. Denoting \mathbf{A} as the weight matrix sampled from posterior distribution, and $\Delta\mathbf{A}$ as the batched noise for sampling \mathbf{A} , the output vector \mathbf{z}_i after applying flipout is:

$$\mathbf{z}_i = \mathbf{W}\mathbf{h}_i \quad (64)$$

$$= \mathbf{W}_0\mathbf{h}_i + \mathbf{B}\mathbf{A}\mathbf{h}_i \quad (65)$$

$$= \mathbf{W}_0\mathbf{h}_i + \mathbf{B}(\mathbf{M} + \Delta\mathbf{A})\mathbf{h}_i \quad (66)$$

$$= \mathbf{W}_0\mathbf{h}_i + \mathbf{B}\mathbf{M}\mathbf{h}_i + \mathbf{B}(\widehat{\mathbf{A}} \circ \mathbf{t}_i \mathbf{s}_i^\top)\mathbf{h}_i. \quad (67)$$

Similarly, for a mini-batch input matrix $\mathbf{H} \in \mathbb{R}^{n \times b}$ with batch size b , we randomly sample two low-rank flipping matrices $\mathbf{S} \in \{-1, +1\}^{n \times b}$ and $\mathbf{T} \in \{-1, +1\}^{b \times r}$. The batched output matrix \mathbf{Z} after applying flipout is then:

$$\mathbf{Z} = \mathbf{W}_0\mathbf{H} + \mathbf{B}(\mathbf{M}\mathbf{H} + [\widehat{\mathbf{A}}(\mathbf{H} \circ \mathbf{S})] \circ \mathbf{T}) \quad (68)$$

$$= \mathbf{W}_0\mathbf{H} + \mathbf{B}(\mathbf{M}\mathbf{H} + [(\mathbf{E} \circ \Omega)(\mathbf{H} \circ \mathbf{S})] \circ \mathbf{T}). \quad (69)$$

Hyperparameter	Model	
	Roberta-base	Llama2-7B
Optimizer	AdamW	
LR Scheduler	Linear	
Warmup Ratio	0.06	
Learning Rate	$5e-4$	$1e-4$
Batch Size	32	4
Max Seq. Len.	512	300
LoRA α	8	16
LoRA r	8	

Table 3: Hyperparameters of LoRA

Hyperparameter	Model	
	Roberta-base	Llama2-7B
Optimizer of KL	SGD	
LR of KL	0.002	0.01
σ_p	0.2	
ϵ	0.05	
γ	8	

Table 4: BLoB-Specific Hyperparameters

B Implementation Details

In this section, we first introduce the implementation details of BLoB in Appendix B.1, including the KL Re-weighting scheme, initialization of the parameters, and learning scheduling, etc. Next, we introduce the two evaluation metrics for uncertainty estimation in Appendix B.2. Finally, we present some statistics of the adopted datasets in Appendix B.3.

B.1 Implementation of BLoB

KL Re-weighting. In mini-batch SGD, the training data \mathcal{D} is randomly divided into M equally sized subsets: $\mathcal{D}_1, \mathcal{D}_2, \dots, \mathcal{D}_M$. For mini-batch $i = 1, 2, \dots, M$, the cost function is:

$$\mathcal{F}(\mathcal{D}_i, \theta) = -\mathbb{E}_{q(\mathbf{W}|\theta)}[\log P(\mathcal{D}_i|\mathbf{W})] + \lambda_i \text{KL}[q(\mathbf{W}|\theta) \parallel P(\mathbf{W})], \quad (70)$$

where $\lambda_i \in [0, 1]$ and $\sum_{i=1}^M \lambda_i = 1$. There are various approaches for controlling the weight of KL divergence. [30] utilizes $\lambda_i = 1/M$, while [11] adopts $\lambda_i = 2^{M-i}/2^M - 1$. In fine-tuning tasks, we found that using a scheduler with $\lambda_i = 2^i/2^M - 1$ performs well. This allows the model to find good fits to the data points within the early stages and then optimize the complexity cost in later stages.

In multiple epochs of mini-batch SGD, larger datasets require more iterations to complete one epoch, resulting in delayed convergence of the complexity cost. To enhance the stability of BLoB’s performance across datasets with varying sizes, we pseudo-rescaled the size of the training dataset to make smaller datasets slightly larger and larger datasets slightly smaller. For the portions of the dataset that required expansion, we incorporated additional mini-batches from subsequent epochs. Conversely, for the datasets needing reduction, we deferred the excess mini-batches to subsequent epochs. We denote the size of original dataset as L_0 , The rescaled dataset size is:

$$L^* = 100 \cdot L_0^{\frac{\pi}{\gamma}}, \quad (71)$$

where γ is a coefficient used to control the scaling magnitude, and we set it to 8 in all experiments.

The pseudo-rescaling does not affect the likelihood cost in practical mini-batch gradient descent. In fact, it only changes the warm-up period in KL reweighting from M to $L^*/\text{batch size}$, thereby facilitating more consistent optimization of the complexity cost across datasets of different sizes.

Additional Details. We initialize standard deviation parameterization matrix \mathbf{G} by element-wise sampling from a uniform distribution with a range of $[\frac{\epsilon}{\sqrt{2}}, \epsilon]$, while keeping the remaining initialization settings consistent with LoRA. To maintain consistency, we use the same learning rate scheduler and warmup ratio for the optimizer of the KL term as we do for the likelihood term. We sample only once during the training process. During inference, we sample N times, then take the average of the logits obtained after passing through the softmax function. Detailed hyperparameter settings are provided in the Table 4. Table 3 provides the hyperparameters for fine-tuning with LoRA shared with other baselines. Our experiments on Llama2-7B were conducted using 2 NVIDIA RTX A5000 GPUs for parallel training, while experiments on RoBERTa-base were conducted using 4 NVIDIA RTX A5000 GPUs for parallel training.

B.2 Evaluation Metrics for Uncertainty Estimation

Negative Log-Likelihood (**NLL**) and Expected Calibration Error (**ECE** [31]) are two prevalent metrics for assessing uncertainty estimation.

NLL calculates the sum of the negative expected log probability of predicting the actual label:

$$\text{NLL} = \sum_{i=1}^N -\log P(y_i), \quad (72)$$

where $P(y_i)$ represents the model’s predicted probability for the true label. This metric prefers models that assign higher probabilities to correct labels. If the model exhibits overconfident in an incorrect prediction, the probability assigned to the correct label will be diminished, thereby increasing the NLL.

On the other hand, ECE measures how well the model’s confidence matches its accuracy. This is done by binning the predictions based on their confidence levels and then computing a weighted average of the absolute difference between accuracy and confidence within each bin:

$$\text{ECE} = \sum_{m=1}^M \frac{|B_m|}{n} |\text{acc}(B_m) - \text{conf}(B_m)|, \quad (73)$$

where $\text{acc}(B_m)$ and $\text{conf}(B_m)$ denote the average accuracy and confidence within bin B_m , respectively. These are given by:

$$\text{acc}(B_m) = \frac{1}{|B_m|} \sum_{i \in B_m} \mathbf{1}(\hat{y}_i = y_i), \quad \text{conf}(B_m) = \frac{1}{|B_m|} \sum_{i \in B_m} P(\hat{y}_i), \quad (74)$$

where $|B_m|$ is the number of samples in bin m . We set $|B_m| = 15$ across all experiments.

B.3 Dataset Details

Table 5 summarizes the size of the training set and the number of labels for each dataset. Table 6 summarizes the prompt templates used for common sense reasoning tasks.

Table 5: Size of the training set and number of labels for each dataset.

	WG-S [81]	ARC-C [18]	ARC-E [18]	WG-M [81]	OBQA [64]	BoolQ [17]	RTE [19]	MRPC [24]	WiC [75]	CoLA [97]
Size of Train. Set	640	1.12k	2.25k	2.56k	4.96k	2.49k	3.67k	5.43k	8.55k	9.43k
Num. of Labels	2	5	5	2	4	2	2	2	2	2

Table 6: Prompt templates for common sense reasoning tasks.

Task	Prompt
Winogrande (WG-S/WG-M)	Select one of the choices that answers the following question: {question} Choices: A. {option1}. B. {option2}. Answer:
ARC (ARC-C/ARC-E), Openbook QA (OBQA), MMLU	Select one of the choices that answers the following question: {question} Choices: A. {choice1}. B. {choice2}. C. {choice3}. D. {choice4}. Answer:
BoolQ	Answer the question with only True or False: {question} Context: {passage}.

Table 7: **Performance of different uncertainty-based methods applied to LoRA on RoBERTa-base pre-trained weights.** The evaluation is undertaken on five GLUE [93] and SuperGLUE [92] tasks, with a shared hyper-parameter setting without using individual validation dataset. “ \uparrow ” and “ \downarrow ” represent that higher and lower values are preferred, respectively. The **boldface** and underline are used to denote the best and runner-up performance, respectively. The asterisk “*” denotes training failure.

Metric	Method	Datasets				
		RTE [19]	MRPC [24]	WiC [75]	CoLA [97]	BoolQ [17]
ACC (\uparrow)	MLE	75.81 \pm 0.78	86.27 \pm 0.69	64.52 \pm 0.91	83.29 \pm 0.16	77.67 \pm 0.51
	MAP	75.81 \pm 2.26	86.36 \pm 0.51	65.46 \pm 1.04	83.00 \pm 0.15	77.69 \pm 0.65
	MCD [29]	75.45 \pm 1.30	88.48 \pm 0.01	68.55 \pm 0.65	83.76 \pm 1.03	77.02 \pm 0.60
	ENS [51, 8, 96]	77.74 \pm 1.10	88.64 \pm 0.37	65.83 \pm 0.41	84.08 \pm 0.44	78.57 \pm 0.36
	BBB [11]	49.46* \pm 2.53	68.38 \pm 0.00	50.57* \pm 1.74	69.13 \pm 0.00	62.16 \pm 0.04
	LAP [108]	76.05 \pm 0.95	86.52 \pm 0.72	64.52 \pm 0.91	83.29 \pm 0.16	77.67 \pm 0.52
	BLoB (N=0)	76.05 \pm 0.17	88.24 \pm 0.00	63.17 \pm 0.22	80.92 \pm 0.70	74.80 \pm 2.10
BLoB (N=5)	74.61 \pm 0.61	88.48 \pm 0.60	64.00 \pm 0.53	80.54 \pm 0.16	74.77 \pm 1.77	
BLoB (N=10)	75.45 \pm 0.51	88.73 \pm 0.35	64.26 \pm 1.00	80.89 \pm 0.24	75.49 \pm 1.60	
ECE (\downarrow)	MLE	20.59 \pm 1.25	11.13 \pm 1.05	25.72 \pm 0.83	10.70 \pm 0.49	10.02 \pm 0.71
	MAP	21.67 \pm 3.25	11.12 \pm 0.45	24.26 \pm 1.17	10.61 \pm 0.49	10.11 \pm 0.62
	MCD [29]	19.29 \pm 1.02	8.55 \pm 0.75	19.24 \pm 1.32	<u>5.38\pm0.62</u>	5.97 \pm 0.67
	ENS [51, 8, 96]	19.47 \pm 0.37	10.13 \pm 0.56	28.62 \pm 0.63	12.44 \pm 0.42	5.98 \pm 0.26
	BBB [11]	2.66* \pm 2.24	6.46 \pm 0.43	2.53* \pm 0.39	3.90* \pm 0.41	5.02* \pm 0.29
	LAP [108]	5.33\pm0.60	6.29 \pm 0.99	11.48\pm0.67	3.13\pm0.28	4.84 \pm 0.15
	BLoB (N=0)	14.64 \pm 0.75	5.61 \pm 0.06	18.93 \pm 1.39	10.90 \pm 0.24	5.80 \pm 0.41
BLoB (N=5)	10.46 \pm 0.61	4.49 \pm 0.32	13.62 \pm 1.18	7.76 \pm 0.21	3.21 \pm 0.13	
BLoB (N=10)	<u>8.97\pm0.98</u>	3.30\pm0.19	<u>13.03\pm0.85</u>	7.83 \pm 0.27	2.90\pm0.12	
NLL (\downarrow)	MLE	1.11 \pm 0.02	0.62 \pm 0.02	1.19 \pm 0.03	0.53 \pm 0.02	0.56 \pm 0.01
	MAP	1.23 \pm 0.10	0.58 \pm 0.04	1.14 \pm 0.06	0.53 \pm 0.00	0.55 \pm 0.02
	MCD [29]	0.86 \pm 0.07	0.39 \pm 0.03	0.84 \pm 0.04	0.39\pm0.01	0.51 \pm 0.01
	ENS [51, 8, 96]	1.04 \pm 0.05	0.63 \pm 0.02	1.70 \pm 0.07	0.62 \pm 0.00	0.48\pm0.00
	BBB [11]	0.69* \pm 0.00	0.63 \pm 0.00	0.69* \pm 0.00	0.62 \pm 0.00	0.67 \pm 0.00
	LAP [108]	0.55 \pm 0.00	0.47 \pm 0.01	0.63\pm0.00	0.48 \pm 0.00	0.53 \pm 0.00
	BLoB (N=0)	0.56 \pm 0.01	0.29 \pm 0.00	0.76 \pm 0.02	0.52 \pm 0.01	0.52 \pm 0.02
BLoB (N=5)	<u>0.50\pm0.01</u>	<u>0.27\pm0.00</u>	0.68 \pm 0.01	<u>0.45\pm0.01</u>	0.51 \pm 0.02	
BLoB (N=10)	0.48\pm0.01	0.26\pm0.00	<u>0.67\pm0.01</u>	0.46 \pm 0.01	<u>0.51\pm0.01</u>	

C Additional Experimental Results

This section provides additional experimental results omitted from the main body of the paper due to space limitations. First, we present the results of BLoB when applied to RoBERTa, another pre-trained language model, in Appendix C.1. Next, in Appendix C.2, we conduct the ablation study on our proposed refinement in BLoB. Then we analyze the memory and training time costs in Appendix C.3. Finally, we provide visualization illustrating our BLoB’s advantage on embedding uncertainty in Appendix C.4.

C.1 Performance of RoBERTa on In-distribution Datasets

We also evaluate different methods on RoBERTa-base, which has approximately $1/50$ the parameter count of Llama2-7B. Table 7 shows the results. Compared to MLE, MAP shows minor improvements in NLL and ECE, while MCD, ENS, and LAP enjoy significant improvements. The convergence difficulty observed with the BBB algorithm is further exacerbated on the smaller model, resulting in significant decreases in ACC across all datasets, and even training failures on RTE and WiC. In contrast, our method demonstrates the best or runner-up performance in uncertainty estimation on almost all datasets. Only a slight decrease in ACC is observed on BoolQ and CoLA. We suspect that such decrease is caused by RoBERTa-base’s small model size compared to the large size of these datasets BoolQ and CoLA (i.e., underfitting). Using a larger pretrained model, e.g., Llama2-7B, would potentially address this issue.

Table 8: **Ablation study of BLoB, applied to LoRA on Llama2-7B pre-trained weights**, where **RW**, **RP**, and **AB** represent our designed techniques of **KL Re-Weighting** (Appendix B.1), **Re-Parameterization** (Sec. 3.3), and **Asymmetric Bayesianization** (Sec. 3.1), respectively. The evaluation is done following Table 1. We set the number of samples during training $K = 1$ and the number of samples during inference $N = 10$ across the variants (denoted by “-”) of the BBB [11] and BLoB for fair comparison. We denote by “*” experiments with the scaled standard deviation matrix. The hyphen “-” in the table denotes training failure caused by “NaN” loss. “ \uparrow ” and “ \downarrow ” indicate that higher and lower values are preferred, respectively. **Boldface** and underlining denote the best and the second-best performance, respectively.

Metric	Method	Techniques			Datasets					
		RW	RP	AB	WG-S [81]	ARC-C [18]	ARC-E [18]	WG-M [81]	OBQA [64]	BoolQ [17]
ACC (\uparrow)	MLE	-	-	-	68.99 \pm 0.58	69.10 \pm 2.84	85.65 \pm 0.92	74.53 \pm 0.66	81.52 \pm 0.25	86.53 \pm 0.28
	BBB- BBB-*	-	-	-	-	-	-	-	-	-
	BBB [11]	-	-	✓	56.54 \pm 7.87	68.13 \pm 1.27	85.86 \pm 0.74	73.63 \pm 2.44	82.06\pm0.59	87.21 \pm 0.22
	BLoB- BLoB-*	✓	✓	✓	69.75\pm0.60	67.91 \pm 1.43	<u>86.03\pm0.74</u>	76.24\pm0.55	<u>81.65\pm0.66</u>	87.23\pm0.42
	BLoB- BLoB-*	✓	✓	-	-	-	-	-	-	-
	BLoB-*	✓	✓	-	69.75\pm0.26	70.27\pm0.48	86.33\pm0.44	74.92 \pm 0.19	81.32 \pm 0.41	86.47 \pm 0.46
	BLoB (Ours)	✓	✓	✓	<u>69.07\pm0.34</u>	68.81 \pm 1.09	85.56 \pm 0.35	<u>73.69\pm0.17</u>	81.52 \pm 0.74	86.99 \pm 0.24
ECE (\downarrow)	MLE	-	-	-	29.83 \pm 0.58	29.00 \pm 1.97	13.12 \pm 1.39	20.62 \pm 0.74	12.55 \pm 0.46	3.18 \pm 0.09
	BBB- BBB-*	-	-	-	-	-	-	-	-	-
	BBB [11]	-	-	✓	21.81 \pm 12.95	26.23 \pm 1.47	12.28 \pm 0.58	15.76 \pm 4.71	11.38 \pm 1.07	3.74 \pm 0.10
	BLoB- BLoB-*	✓	✓	✓	26.60 \pm 0.78	26.24 \pm 0.94	11.53 \pm 0.52	18.05 \pm 0.76	12.36 \pm 0.42	3.05 \pm 0.09
	BLoB- BLoB-*	✓	✓	-	-	-	-	-	-	-
	BLoB-*	✓	✓	-	16.59 \pm 0.57	<u>13.85\pm1.06</u>	5.93 \pm 0.63	8.33 \pm 0.78	4.77 \pm 0.26	1.18\pm0.20
	BLoB (Ours)	✓	✓	✓	<u>9.35\pm1.37</u>	9.59\pm1.88	3.64\pm0.53	3.01\pm0.12	<u>3.77\pm1.47</u>	<u>1.41\pm0.19</u>
NLL (\downarrow)	MLE	-	-	-	3.17 \pm 0.37	2.85 \pm 0.27	1.17 \pm 0.13	0.95 \pm 0.07	0.73 \pm 0.03	0.32 \pm 0.00
	BBB- BBB-*	-	-	-	-	-	-	-	-	-
	BBB [11]	-	-	✓	1.40 \pm 0.55	2.23 \pm 0.04	0.91 \pm 0.06	0.84 \pm 0.15	0.66 \pm 0.05	0.31\pm0.00
	BLoB- BLoB-*	✓	✓	✓	1.96 \pm 0.20	2.31 \pm 0.13	0.84 \pm 0.03	0.87 \pm 0.01	0.68 \pm 0.00	0.31\pm0.00
	BLoB- BLoB-*	✓	✓	-	-	-	-	-	-	-
	BLoB-*	✓	✓	-	<u>0.80\pm0.02</u>	<u>0.91\pm0.04</u>	0.46 \pm 0.01	<u>0.55\pm0.01</u>	<u>0.51\pm0.00</u>	<u>0.32\pm0.00</u>
	BLoB (Ours)	✓	✓	✓	0.63\pm0.01	0.78\pm0.02	0.40\pm0.01	0.54\pm0.00	0.50\pm0.01	0.31\pm0.00

C.2 Ablation Study

We perform an ablation study on the Llama2-7B model to showcase the effects of a range of techniques we designed: **KL Re-Weighting** (RW, Appendix B.1), **Re-Parameterization** (RP, Sec. 3.3), and **Asymmetric Bayesianization** (AB, Sec. 3.1). In the scenarios w/o AB, we Bayesianize both matrices, \mathbf{A} and \mathbf{B} . In practice, using identical initialization and prior for the standard deviation matrix \mathbf{G} of the variational distribution on both \mathbf{A} and \mathbf{B} leads to training failures caused by “NaN” loss across all datasets; this is consistent with the findings in Sec. 3.1. As a solution, we introduce a scaled standard deviation matrix $\mathbf{G}/_{100}$ on \mathbf{B} to alleviate early-stage fluctuations. Nevertheless, it is important to note that not using AB incurs double the additional memory cost and more than doubles the total training time, as described in Appendix C.3.

As demonstrated in Table 8, BBB w/o AB fails to converge due to the unbounded NaN loss, which cannot be solved by using scaled standard deviation. By introducing **KL Re-Weighting**, **Re-Parameterization**, and scaled standard deviation, **BLoB** w/o AB achieves the runner-up performance and improves accuracy on small datasets. However, **BLoB** with all techniques achieves the best ECE and NLL with minimal additional computational cost.

C.3 Memory and Training Time Cost

By introducing an additional standard deviation matrix $\mathbf{\Omega}$ of the same size as the LoRA \mathbf{A} matrix, the number of trainable parameters in **BLoB** increases by half compared to LoRA. In the case of **BLoB** w/o **Asymmetric Bayesianization** (AB), the number of trainable parameters are twice as many as those

Table 9: **A comparison of training time and memory cost between standard LoRA, BLoB without AB (Asymmetric Bayesianization), and BLoB.** The evaluation is based on fine-tuning for 5,000 steps on the Llama2-7B model.

Metric	Method	Datasets					
		WG-S [81]	ARC-C [18]	ARC-E [18]	WG-M [81]	OBQA [64]	BoolQ [17]
Time (Seconds) (↓)	Standard LoRA	1544	1681	1655	1537	1972	3221
	BLoB without AB	3211	4612	4513	3147	4511	8709
	BLoB	1812	1975	1957	1817	2281	3733
Memory (MB) (↓)	Standard LoRA	14688	16870	17044	14710	14984	20784
	BLoB without AB	15054	19746	19954	15300	16489	26128
	BLoB	15015	18863	19015	15015	15890	23552

in LoRA. The calculation of KL divergence and the inclusion of the additional standard deviation matrix in the likelihood loss computation result in additional forward and backward propagation time. We conduct parallel training using two NVIDIA RTX A5000 GPUs to observe the differences in GPU memory cost and training time between BLoB and standard LoRA fine-tuning on the Llama2-7B model. The results are shown in Table 9. BLoB increases memory cost by only about 3% to 13% compared to LoRA, with training time increased by about 15%. However, BLoB w/o AB doubles the increase of memory cost (LoRA as the baseline) and more than doubles the total training time.

C.4 Embedding Uncertainty of BLoB: A Preliminary Visual Study

Estimating the uncertainty of LLMs in the embedding space has recently garnered significant attention in the community [13]. Expressing models’ uncertainty via their generated embeddings can benefit both discriminative (the focus of this paper) and generative models. In this section, we present a preliminary study on uncertainty estimation in the embedding spaces of different models, as illustrated in Fig. 3. We compare BLoB with two baseline models, BBB and MCD, which can generate embedding samples and effectively estimate uncertainty. We exclude LAP from this section due to its excessive memory consumption, which consistently results in Out-Of-Memory (OOM) errors during inference.

For each input sequence s , we use the last token’s embedding generated by the final transformer block in Llama2-7B as the final embedding. Given the weights \mathbf{W} , we denote the embedding as $\phi(s; \mathbf{W})$. Generally, three types of embeddings can be generated using the Bayesian approach:

- (a) Embeddings generated by the mean of the weights (these embeddings are shown as “★” in Fig. 3):

$$\phi(s; \mathbb{E}_{\mathbf{W} \sim q(\cdot|\theta)}[\mathbf{W}]) = \phi(s; \mathbf{W}_0 + \mathbf{B}\mathbf{M}). \quad (75)$$

- (b) Embedding samples generated by sampling different weights from the approximate posterior, whose distribution is plotted by the solid line (—).

- (c) The expectation of the embedding, which is approximated by averaging the sampled embeddings:

$$\mathbb{E}_{\mathbf{W} \sim q(\cdot|\theta)}[\phi(s; \mathbf{W})] \approx \frac{1}{N} \sum_{n=1}^N \phi(s; \mathbf{W}_0 + \mathbf{B}(\mathbf{M} + \mathbf{E}_n \circ \Omega)), \quad (76)$$

where N denotes the number of samples during inference, and \mathbf{E}_n denotes the n -th sampled noise for the weight matrix. We show this expectation as “▼” in Fig. 3.

To visually demonstrate the confidence calibration effect of the Bayesian treatment, we adopt the following pipeline of visualization, which we believe can be further applied in visualizing other frameworks’ embedding uncertainty quality.

- (1) Acquire high-dimensional embeddings produced by the weight mean for the given test dataset, as described in (a) and Eqn. 75 above.
- (2) Use Linear Discriminant Analysis (LDA) [10] to project these high-dimensional embeddings into a low-dimensional 2D space.

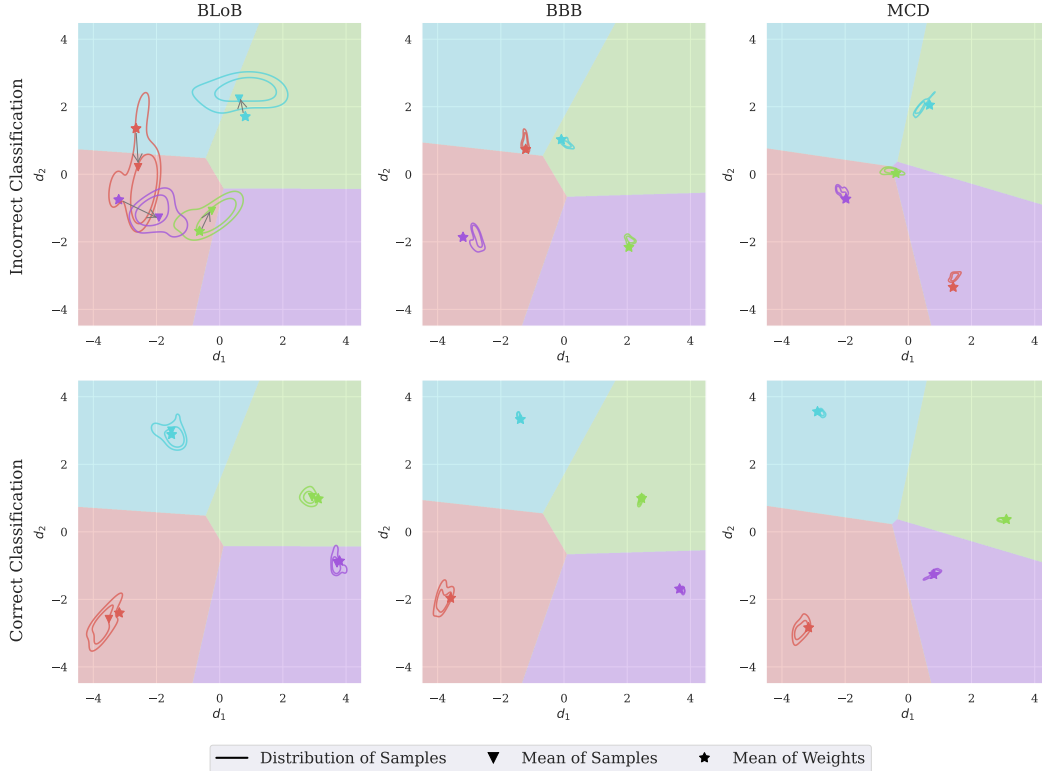


Figure 3: **Visualization of embedding uncertainty quality for different methods.** The model is fine-tuned for 5,000 steps on the Llama2-7B. The two contour lines represent the probability mass of 0.5 and 0.75, respectively.

- (3) In the 2D space, fit a logistic regression model to mimic the decision regions and color them based on the true labels.
- (4) Sample weights 10 times from the approximate posterior, generate the embeddings, and project them into the same 2D space using the previously learned LDA. Use Kernel Density Estimation (KDE) [78, 73] to show their distributions, as described in (b) above.
- (5) Average the sampled embeddings for each example and visualize them in the 2D space, as described in (c) and Eqn. 76 above.

In Fig. 3, we show 4 correct and incorrect predictions made by each model. Ideally, a model with better uncertainty estimation should produce lower level of uncertainty (**smaller embedding variance**, i.e., smaller contours, and **further away from the decision boundary**) for correct predictions, and higher level of uncertainty (**larger embedding variance**, i.e., larger contours, and **closer to the decision boundary**). From the figure, we have the following observations:

- All three Bayesian approaches produce higher embedding variance for incorrect predictions and lower embedding variance for correct predictions. However, BLoB achieves significantly larger embedding variance compared to the baselines, consistent with the quantitative evaluation shown in Table 1. BLoB’s produced variance is higher for the incorrect predictions, demonstrating its accurate uncertainty estimation even in the embedding space.
- In BLoB, the mean embedding produced by sampling weights from the approximate posterior is closer to the decision boundary than the embedding generated by the mean of weights ($\star \rightarrow \blacktriangledown$). This effect is most apparent when the prediction is incorrect, consistent with the quantitative results yielded from the final softmax layer of the model. Again, this demonstrates BLoB’s Bayesian inference can bring the final prediction closer to the ground truth.